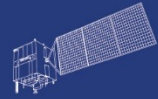


HY



HJ-1AB



CBERS



Gaofen



Beijing-2



Sentinel-1



Sentinel-2



Sentinel-3



Sentinel-5p



Aeolus

2023 DRAGON 5 SYMPOSIUM
3rd YEAR RESULTS REPORTING
11-15 SEPTEMBER 2023

[ID. 59193]

**[Innovative User-relevant Satellite Products
for Coastal & Transitional Waters]**

13 SEPTEMBER 2023

ID. 59193

Project Title: Innovative User-relevant Satellite Products for Coastal & Transitional Waters

Principal Investigators:

Pi China: Prof. **Junsheng Li**, Aerospace Information Research Institute, Chinese Academy of Sciences, China

PI Europe: Prof. **Evangelos Spyrakos**, Earth and Planetary Observation Science, University of Stirling, UK

Co-authors: Jusheng Li, Evangelos Spyrakos, Shenglei Wang, Conor McGlinchey, Yingcheng Lu, Jesus Torres Palenzuela, Saojie Sun, Luis Gonzalez Vilas, Adriana Constantinescu, Adrian Stanica, Mortimer Werther, Dalin Jiang, Andrew Tyler

Presented By: Junsheng Li

- Introduction of the project's information
- Recent progress of the project
 1. Key issues in ocean colour remote sensing
 2. Oil spills detection
 3. Water quality parameter retrieving
- Summary and outlook

Title: Innovative user-relevant satellite products for coastal and transitional waters

Scientific objectives:

- The project aims to build upon recent progress in the realms **of retrieval algorithm development of innovative biogeochemical parameters**, and to exploit the potential capacities offered by the **latest generation of EO data from Europe and China**.
- The objective of this project is **to develop and validate innovative user-relevant water quality monitoring products** for coastal and transitional waters based on EO data, and to support and improve the **water ecosystem services, sustainable management and security**.

Work Plans

WP1. Data acquisition:

- 1.1 In-situ data acquisition from existing dataset and field campaigns
- 1.2 EO data acquisition

WP2. Innovative water quality algorithms development and validation

- 2.1 Phytoplankton size class (PSC)
- 2.2 Primary production (PP)
- 2.3 Harmful algal blooms (HABs) of specific toxic species
- 2.4 Marine oil spill (MOS)

WP3. Algorithm implementation and product generation

WP4. Product scientific and practical value demonstration

Expected results

1. **Newly developed and validated algorithms** for the retrieval of phytoplankton size classes (PSC), primary production (PP), harmful algal blooms (HABs) of specific toxic species, marine oil spill (MOS) from satellite.
2. **Long time series products** of PSC, PP, HABs, and MOS, and related statistics for the regions of interest using satellite data.
3. **Analysis of coastal environment change trends and driving forces** in regional environments, based on a combination of the derived innovative parameters, climate change and anthropogenic perturbations.
4. **Co-authored publications** to demonstrate the algorithms development and validation, and the spatiotemporal changes quantified and the environmental driving factors.

Data access (list all missions and issues if any). NB. in the tables please insert cumulative figures (since July 2020) for no. of scenes of high bit rate data (e.g. S1 100 scenes). If data delivery is low bit rate by ftp, insert “ftp”

ESA /Copernicus Missions	No. Scenes	ESA Third Party Missions	No. Scenes	Chinese EO data	No. Scenes
1. Sentinel-2 MSI	500	1. Planet Super Doves	20	1. HY1C/D UVI	10
2. Sentinel-3 OLCI	500	2.		2. GF5/02 AHSI	10
3.		3.		3.	
4.		4.		4.	
5.		5.		5.	
6.		6.		6.	
Total:		Total:		Total:	
Issues:		Issues:		Issues:	

Name	Institution	Poster title	Contribution including period of research
Conor Ross McGlinchey	University of Stirling, UK	Characterising and Monitoring Phytoplankton Properties from Satellite Data	Started his PhD in October 2022

Name	Institution	Poster title	Contribution including period of research
Shenglei Wang	Aerospace Information Research Institute, Chinese Academy Of Sciences, China	Water colour from Sentinel-2 MSI data for monitoring large rivers: Yangtze and Danubes	2021-now Satellite-based Inland Water Colour Variation Analysis

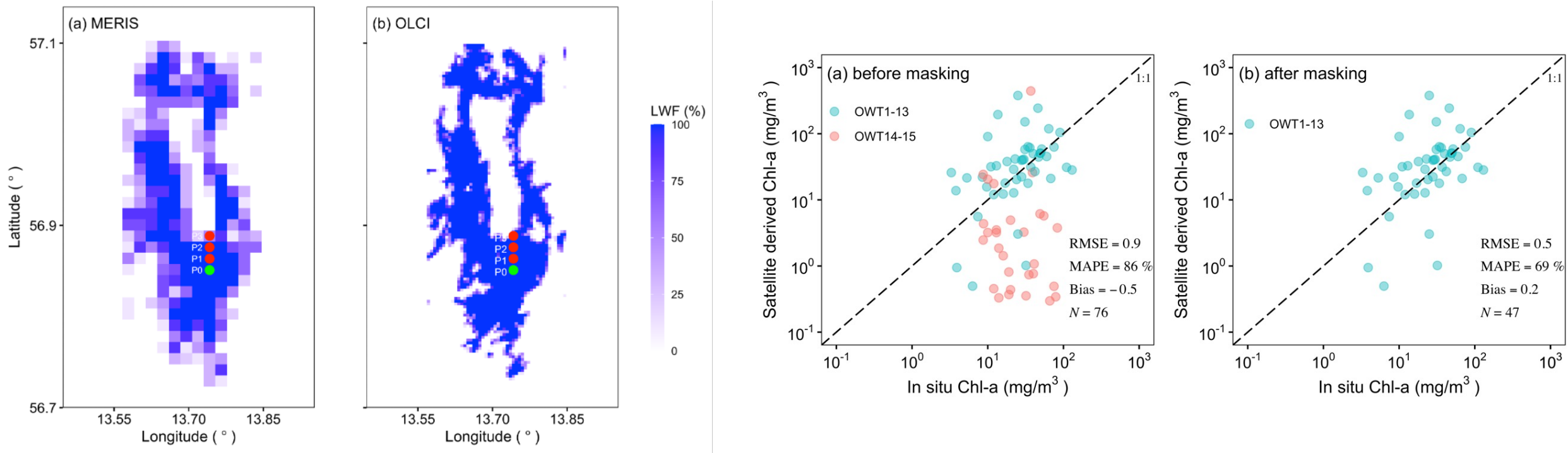
- Introduction of the project's information
- Recent progress of the project
 1. Key issues in ocean colour remote sensing
 2. Oil spills detection
 3. Water quality parameter retrieving
- Summary and outlook

- **Adjacency effects** in nearshore ocean colour data
- **Uncertainty estimates** in ocean colour products

Authors:

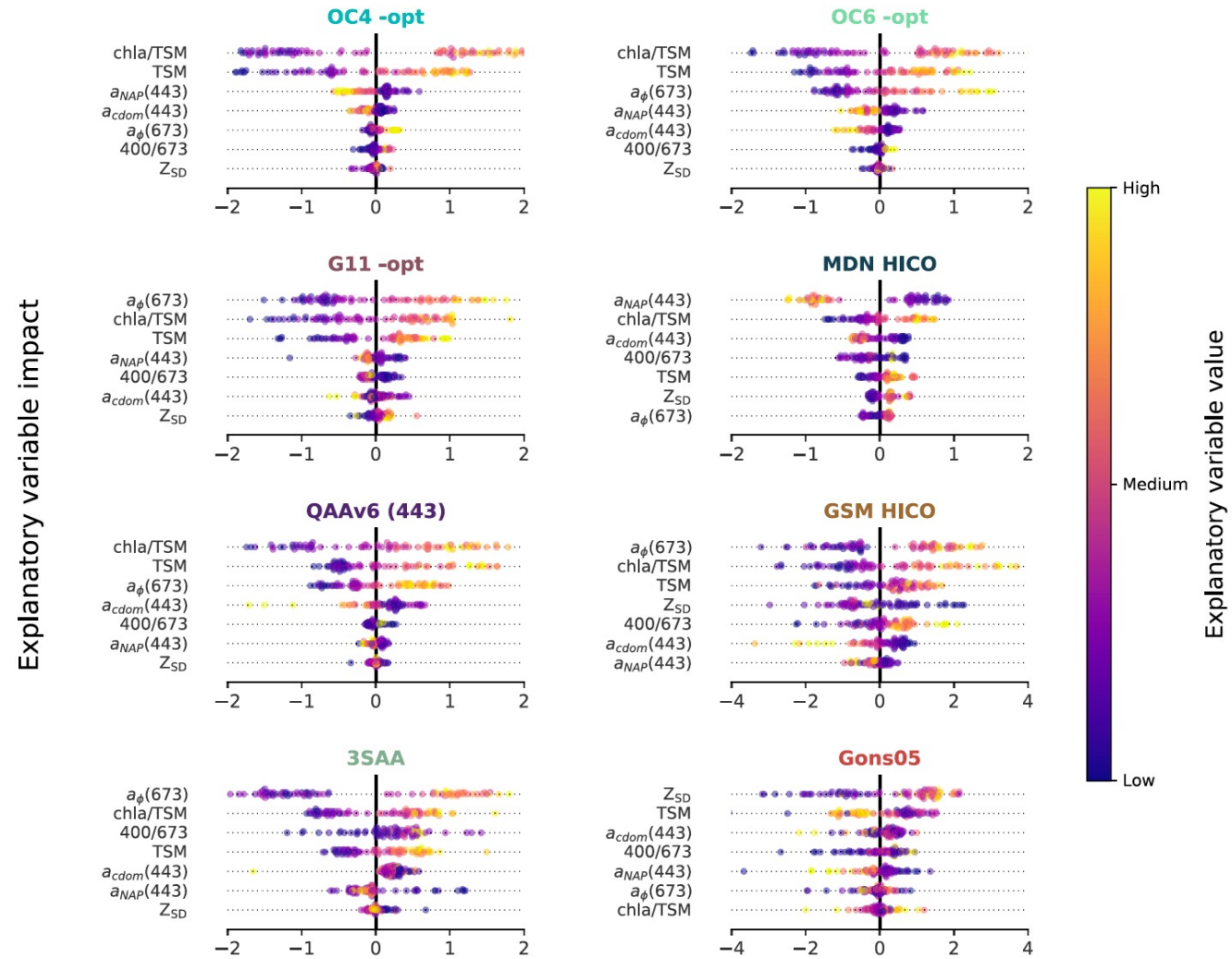
**Evangelos Spyrakos, Conor McGlinchey, Jesus Torres Palenzuela, Luis Gonzalez Vilas,
Adriana Constantinescu, Adrian Stanica, Mortimer Werther, Dalin Jiang, Andrew Tyler**

A new method was developed to identify the effects of the adjacent land on ocean colour products. The Chla retrieval before and after the adjacency effects masking is very different.



Retrieval uncertainty

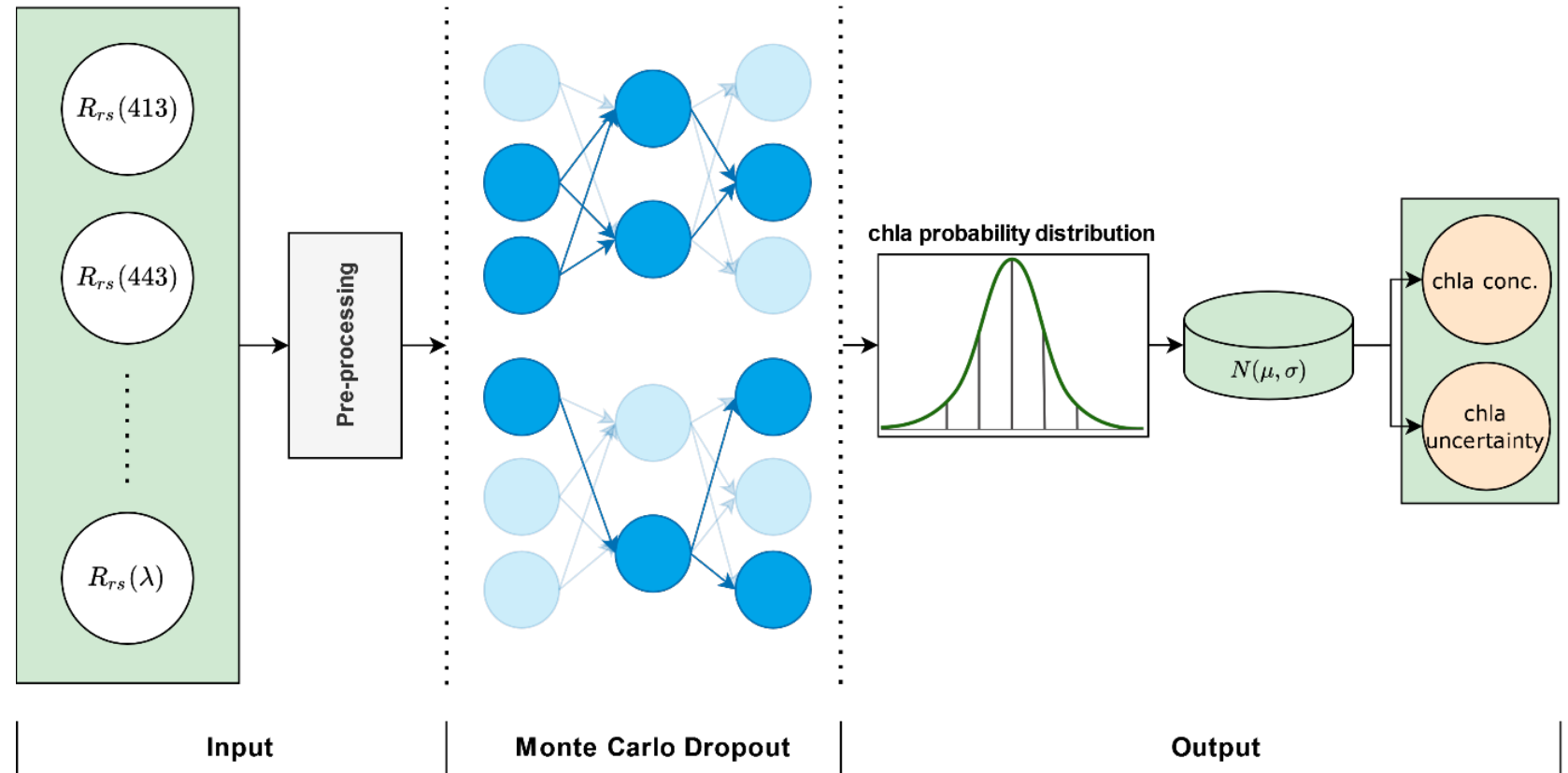
The Chla retrieval uncertainty of most semi-analytical algorithms was primarily determined by phytoplankton absorption and composition.



SHAP values

Retrieval uncertainty

Machine learning Chla algorithms showed relatively high sensitivity to light absorption by coloured dissolved organic matter (CDOM) and non-algal pigment particulates (NAP).



- Introduction of the project's information
- Recent progress of the project
 1. Optical remote sensing image preprocessing
 2. Oil spills detection
 3. Water quality parameter retrieving

- Detection of oil spills using **ultraviolet remote sensing**
- Detection of oil spills in northern South China Sea using **Landsat-8 OLI data**

Detection of oil spills using ultraviolet remote sensing

Ziyi Suo¹, Yingcheng Lu^{1, *}, Jiangqiang Liu², Jing Ding², Dayi Yin³, Feifei Xu³, Junnan Jiao¹

1 International Institute for Earth System Science, Nanjing University

2 Key laboratory of Space Ocean Remote Sensing and Application, National Satellite Ocean Application Service, Ministry of Natural Resources

3 Key Laboratory of Infrared System Detection and Imaging Technology, Shanghai Institute of Technical Physics, Chinese Academy of Sciences

1 Introduction

■ Research background – Source of marine oil

- Human activities (94%)
- Natural hydrocarbon leakage (6%)



Platform explosion



Oil tanker capsized



Pipeline leakage



Natural leakage

1 Introduction

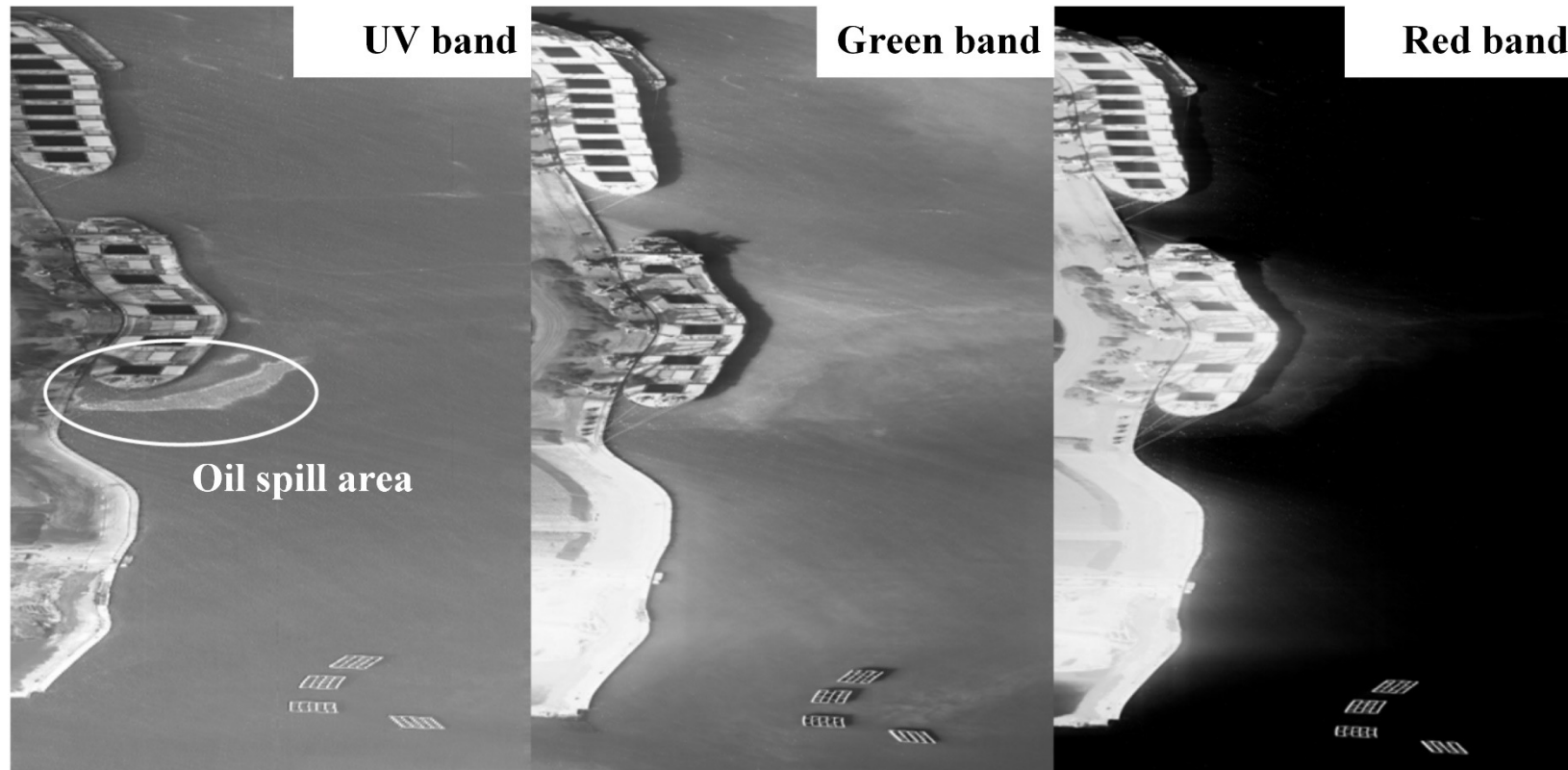
■ Research background – Remote sensing of marine oil spills

Technologies	Characteristics
SAR	All-day and all-weather observation; Lack of diagnostic features
Optical	Distinguishable reflectance shapes to classify oil types and estimate oil concentration; Suffering from clouds
Thermal	Indicating oil contents; Unable to classify oil types
Ultraviolet (UV)	Airborne: Oil slicks are sensitive to UV radiance, appearing positive contrast with seawater (<i>Yin et al., 2010</i>). How is Spaceborne UV imager?

1 Introduction

■ Research background – Remote sensing of marine oil spills

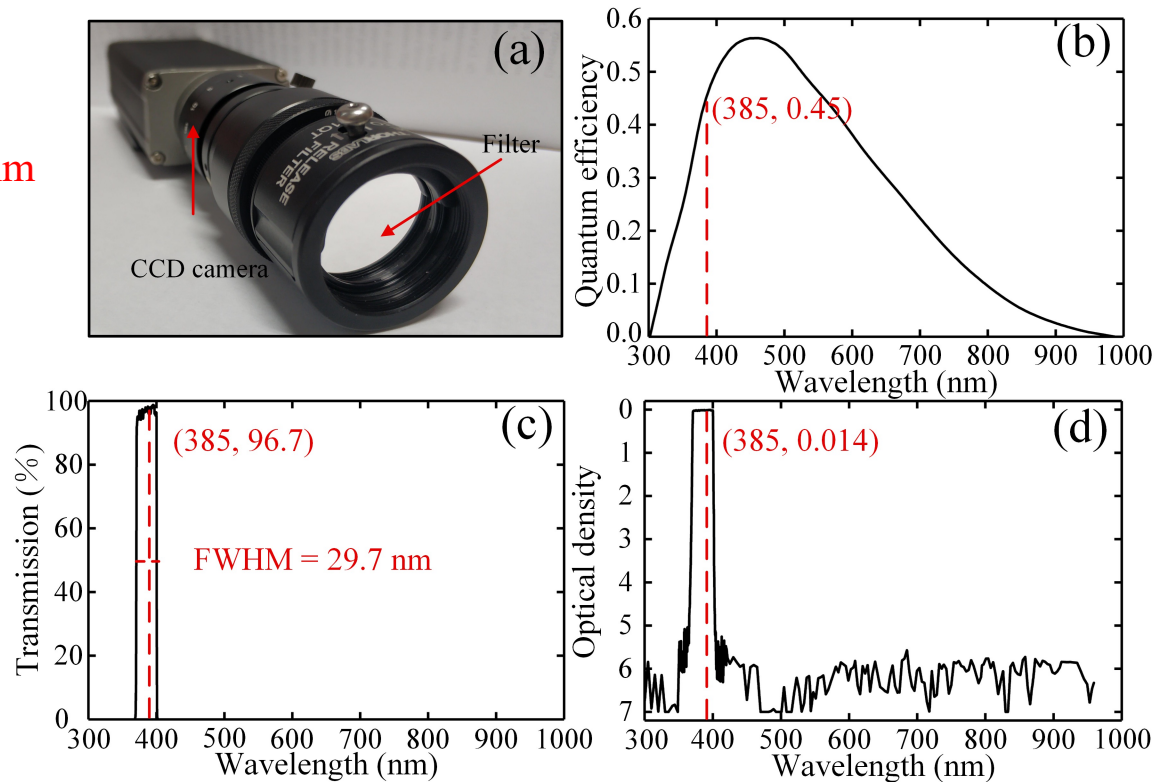
HY-1C/D satellites are the first operational ocean color satellite of China, the Ultraviolet Imager onboard provides the only data for marine environment observation at 355 and 385 nm.



2 Data and methods

■ Ground-based experiment

Filter: 385nm

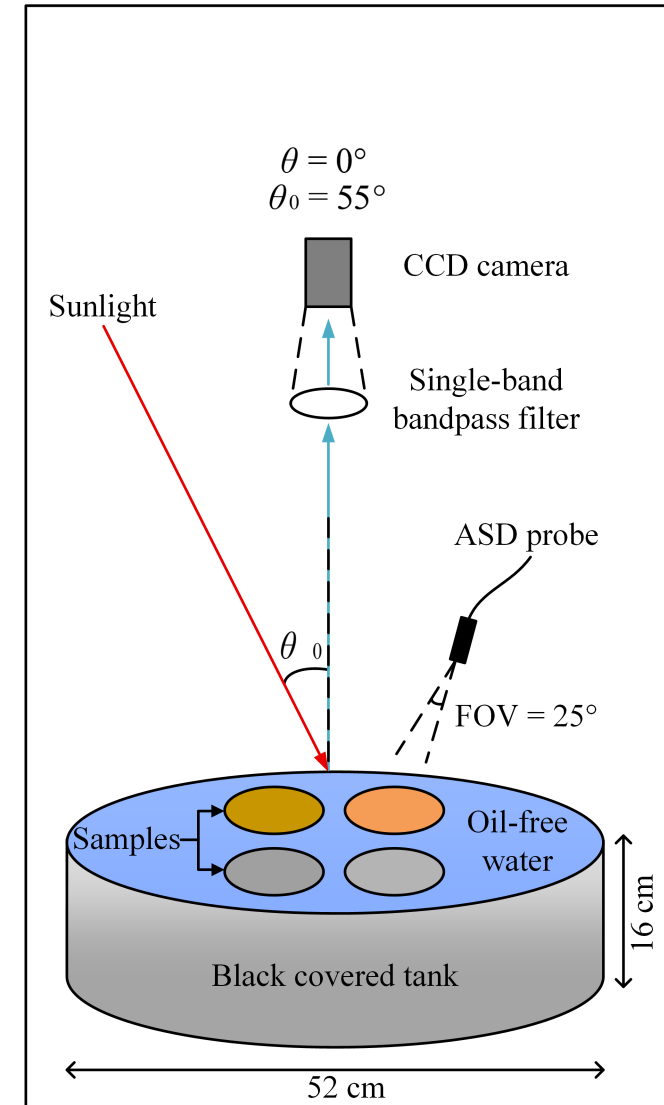


$$OD = \lg(1/T)$$

Oil samples:

- ① Water-in-oil (WO) emulsion (75%);
- ② Oil-in-water (OW) emulsion (1%);
- ③ Thin oil slick;
- ④ Thick oil slick

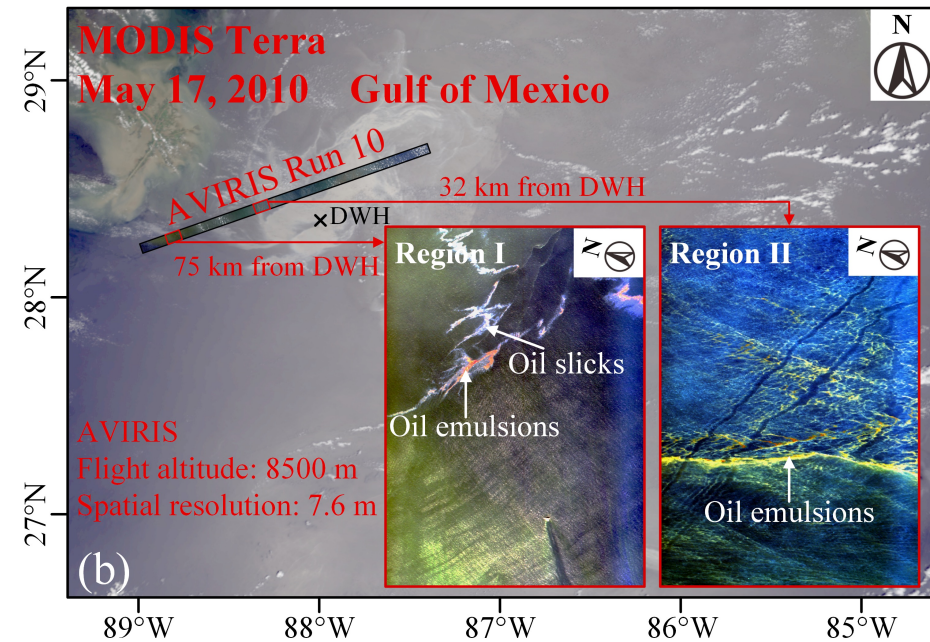
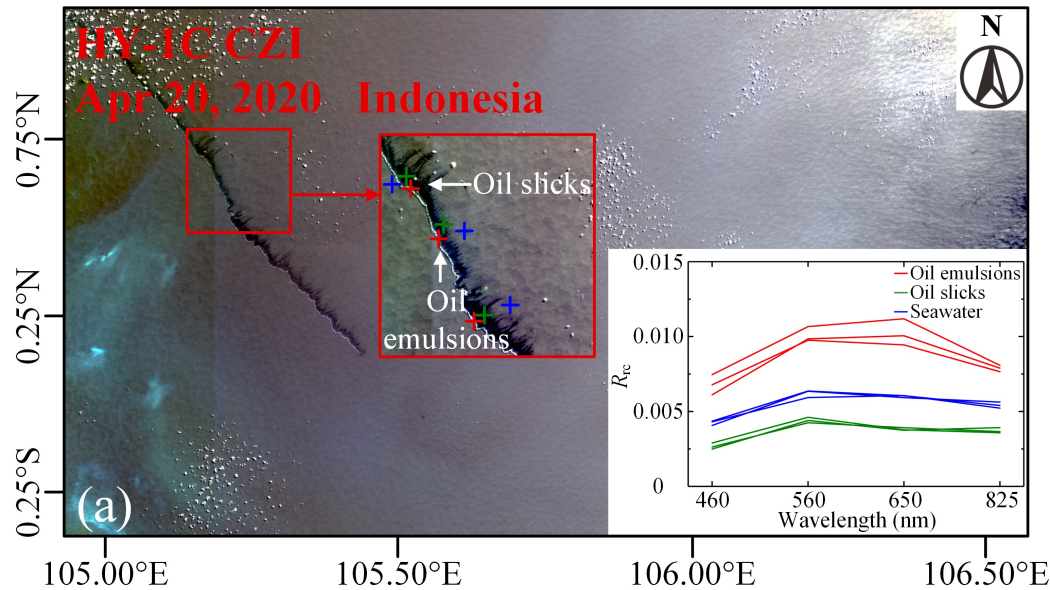
(Lu et al., RSE, 2019)



Suo et al., Optics Express, 2021

2 Data and methods

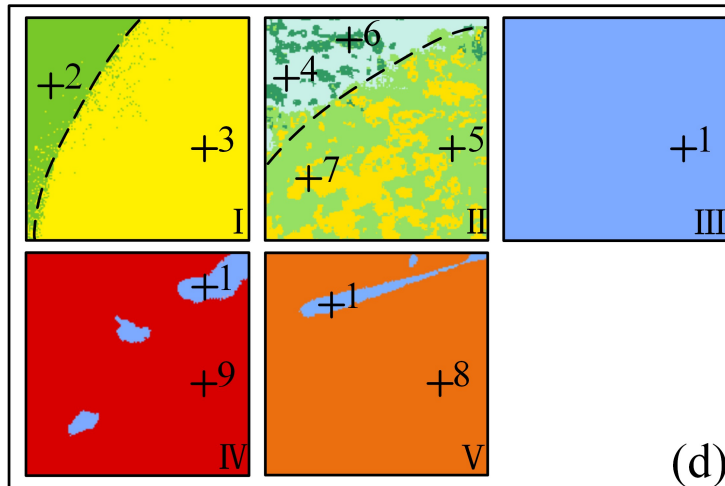
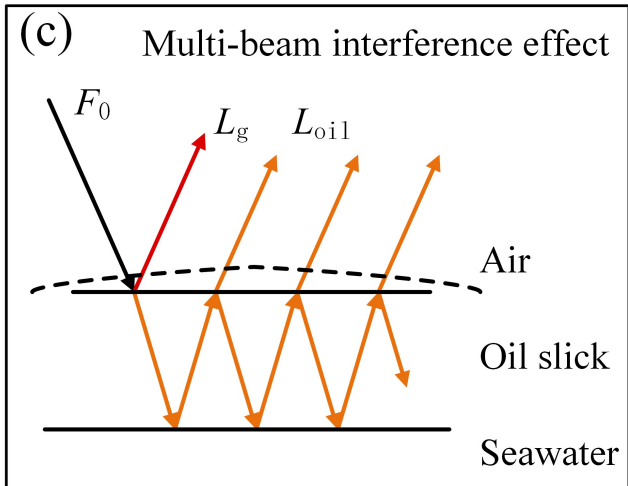
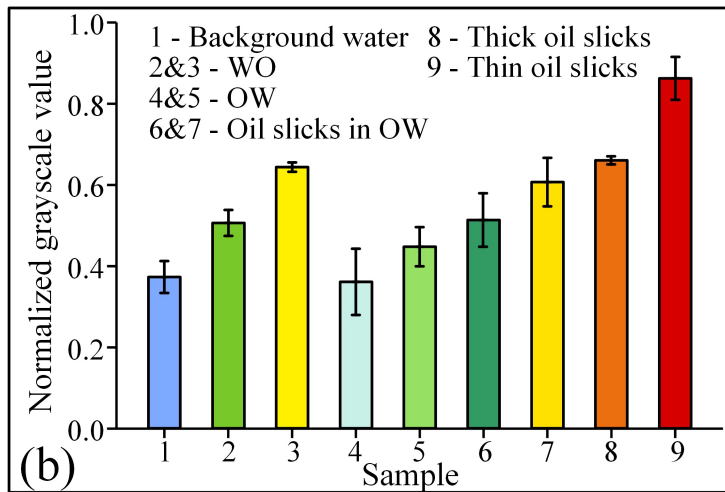
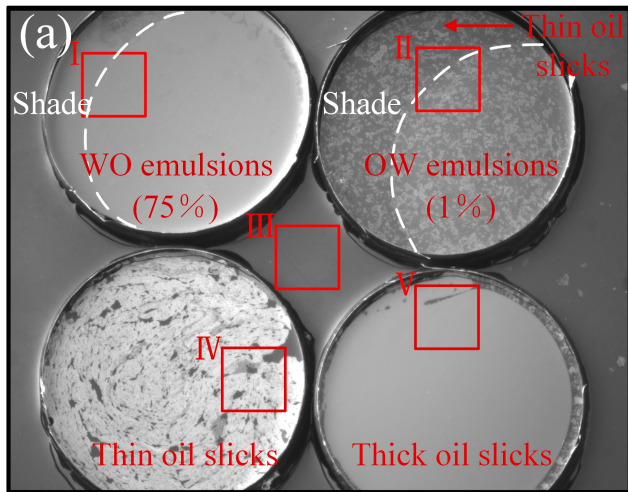
Spaceborne and airborne images



Parameters	HY-1C/D UVI	AVIRIS
Platform	Spaceborne	Airborne
Center wavelength	355 & 385 nm	380.21 nm
Spatial resolution	~1100 m	7.6 m
Flight height	782 km	8.5 km

3 UV reflection characteristics of weathered oils

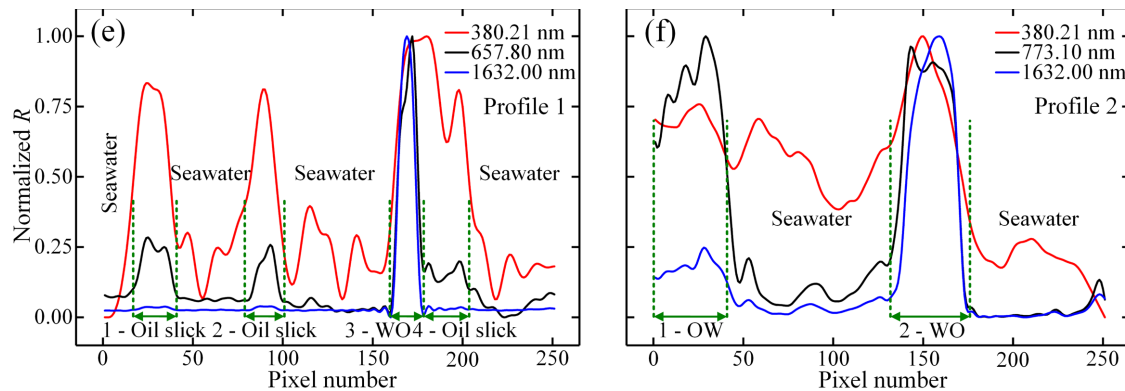
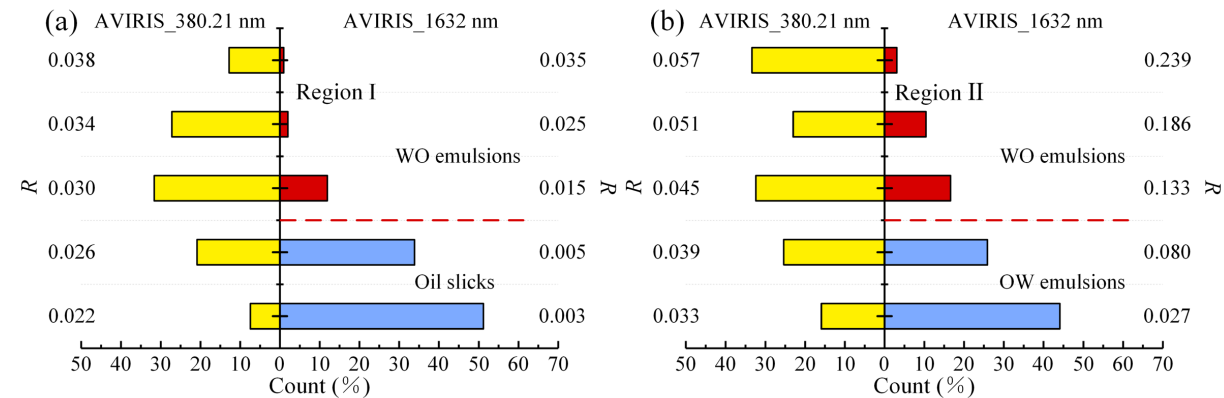
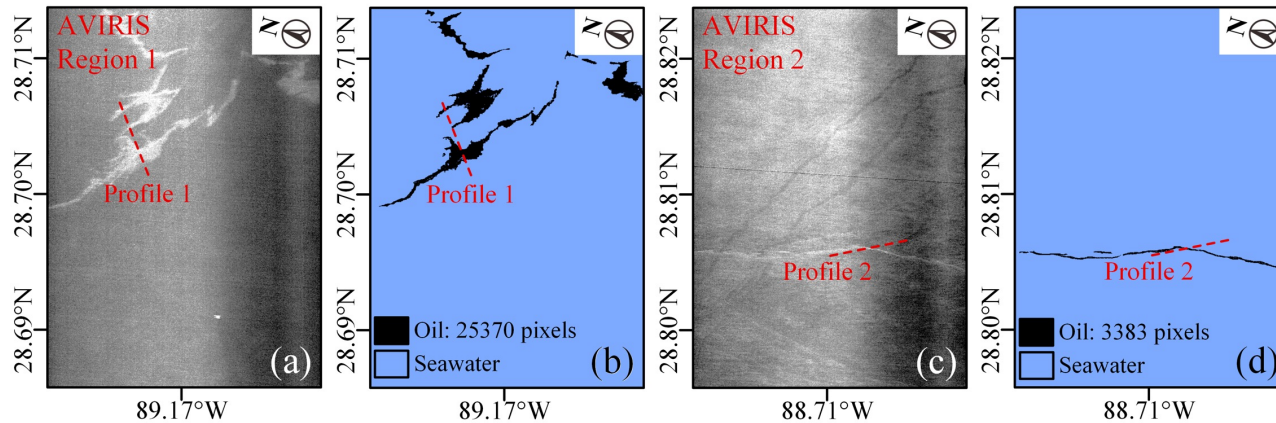
■ UV reflection characteristics of weathered oils



- Oil slick appears positive contrast in UV image as the surface interference light raises its reflectance;
- All the oils appear brighter than background water;
- UV band of 385 nm can hardly be used to classify oil types as oils are close in UV brightness

4 Scale effect of UV remote sensing of marine oil spills

■ Proof of spilled oils in airborne UV images



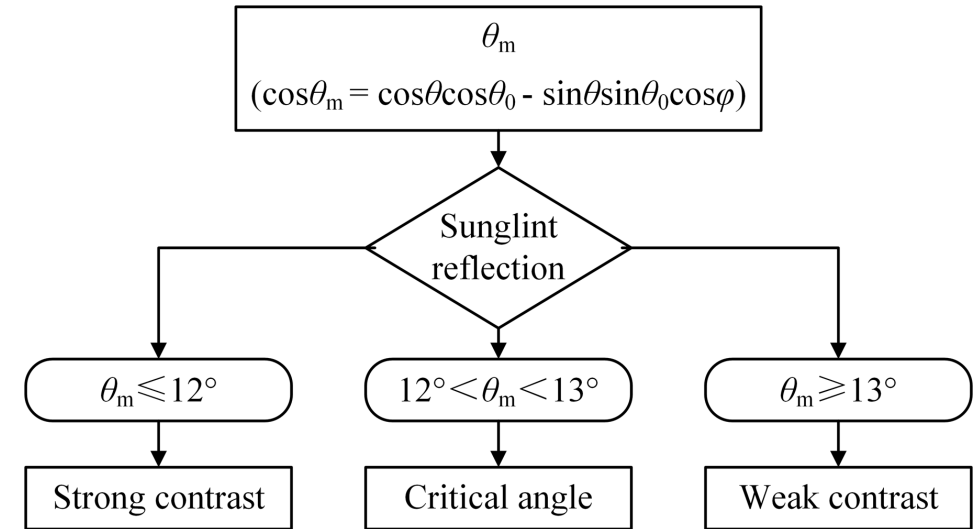
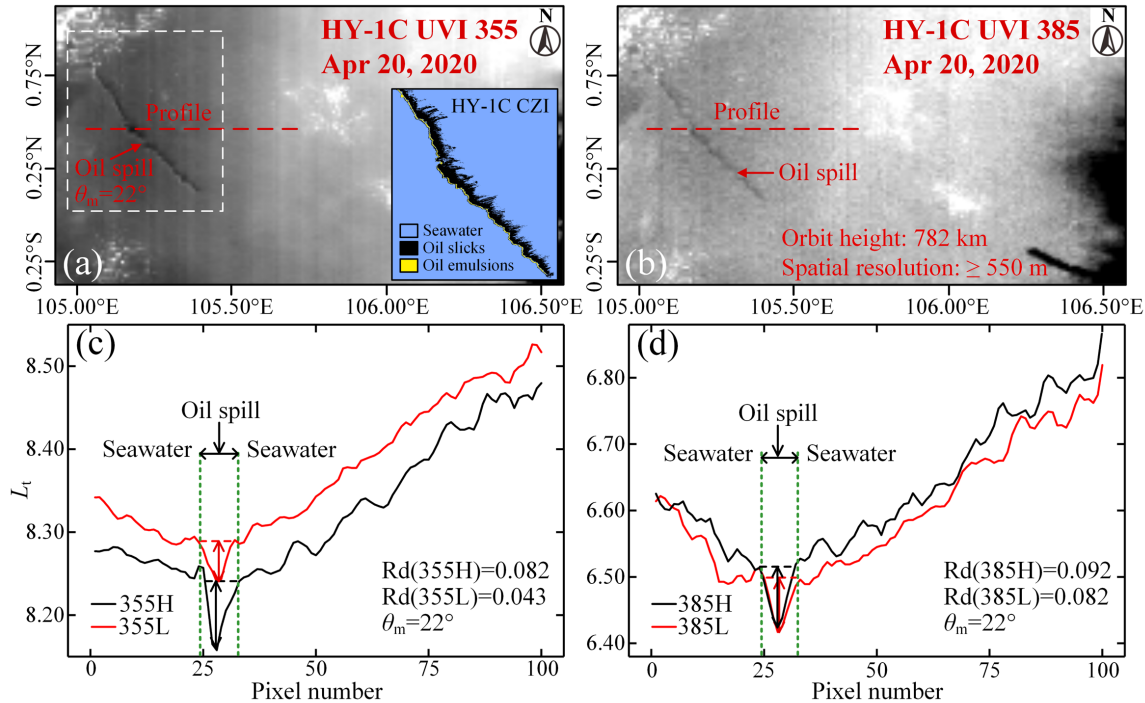
- Oil spills still appear **bright contrast with seawater** in AVIRIS UV images with **high spatial resolution**;
- Oil slicks and WO show **spectral response consistency** in UV and characteristic bands;
- Oil types **can not be classified** using only UV band

What features will oil spills show in spaceborne UV images?

Can the surface interference light still be observed?

4 Scale effect of UV remote sensing of marine oil spills

UV detection of spilled oils in UVI images under sunglint



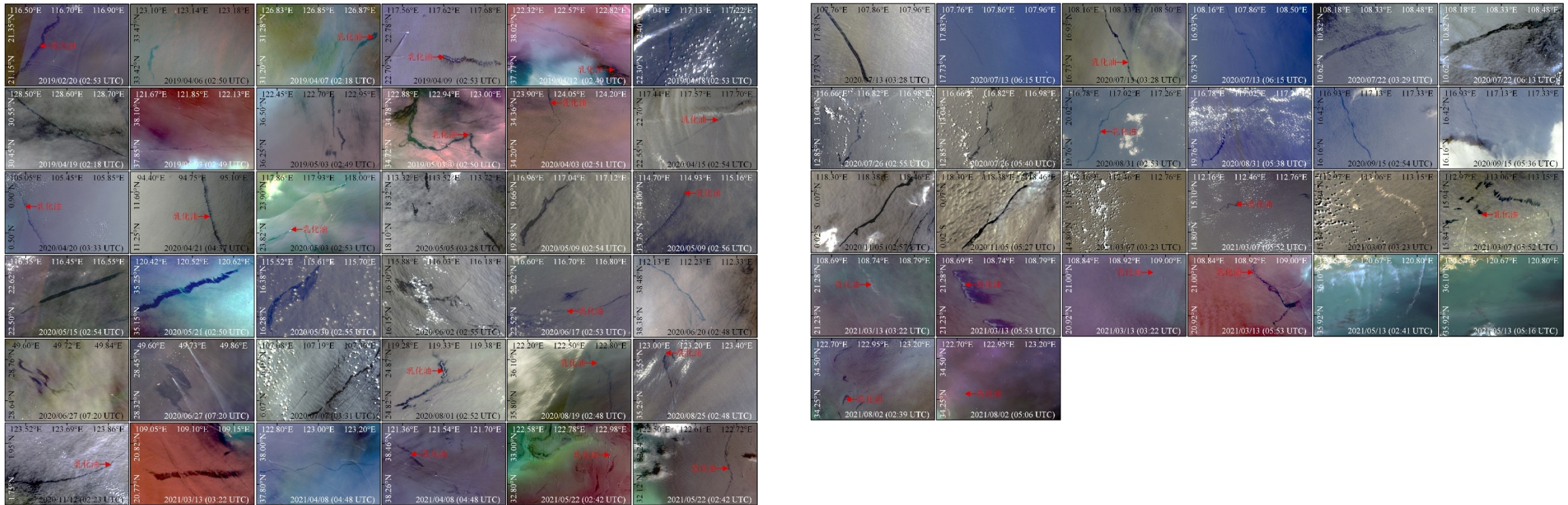
$$\cos\theta_m = \cos\theta\cos\theta_0 - \sin\theta\sin\theta_0\cos\varphi$$

θ , θ_0 and φ are satellite/solar zenith angle and relative azimuth angle.

- Oil spills and seawater show **negative contrast** in UVI images **under weak sunglint**;
- For spaceborne UV images with **low spatial resolution**, **sunglint reflection** determines the image features of spilled oils.

5 Sunlight requirement for spaceborne UV detection of spilled oils

■ Sunlight reflection and detectability of oil spills



HY-1C/D satellites have detected 57 oil spill incidents from 2018 to 2021.

35 of them can be detected by COCTS, however, only 13 of them can also be detected in UVI images.

How to determine the minimum sunlight strength for oil spill detection in UVI images?

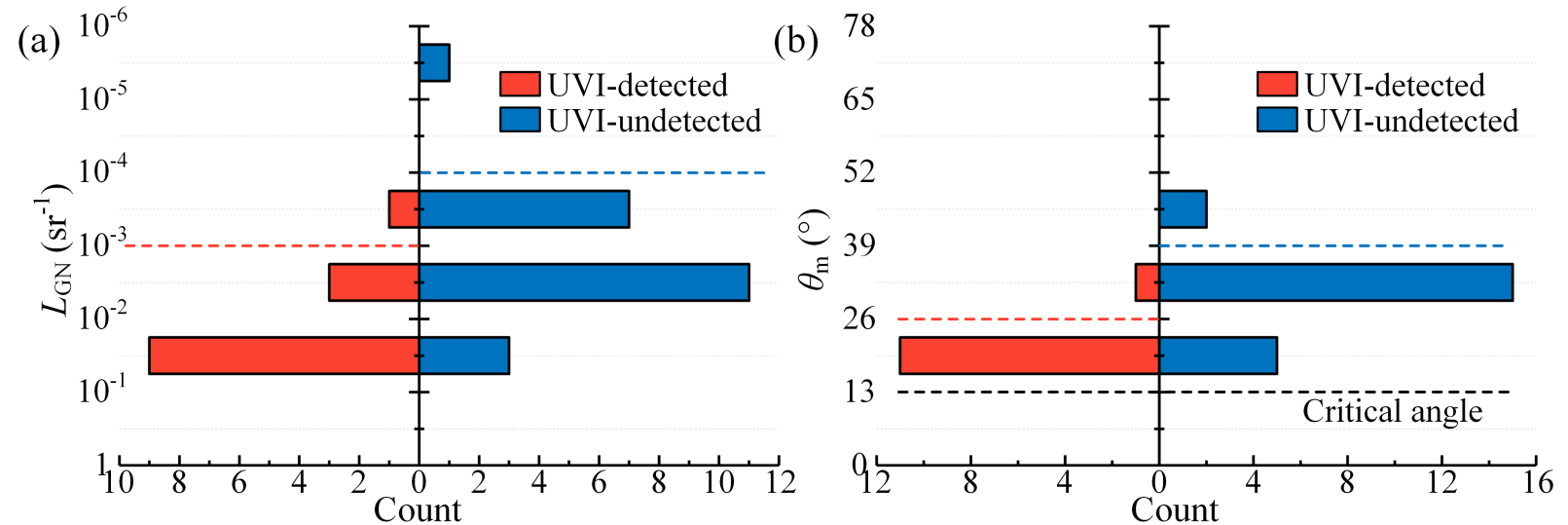
5 Sunglint requirement for spaceborne UV detection of spilled oils

■ Sunglint reflection and detectability of oil spills

CZI (RGB)	COCTS (RGB)	UVI (355 nm)	UVI (385 nm)	
				(a) 2019/02/20 $\theta_m = 38^\circ$ $L_{GN} = 1.5E-4 \text{ sr}^{-1}$
				(b) 2020/04/20 $\theta_m = 22^\circ$ $L_{GN} = 1.2E-2 \text{ sr}^{-1}$
				(c) 2020/07/22 $\theta_m = 18^\circ$ $L_{GN} = 2.5E-2 \text{ sr}^{-1}$
				(d) 2020/08/31 $\theta_m = 34^\circ$ $L_{GN} = 6.1E-4 \text{ sr}^{-1}$
				(e) 2020/09/15 $\theta_m = 26^\circ$ $L_{GN} = 5.4E-3 \text{ sr}^{-1}$
				(f) 2021/03/07 $\theta_m = 36^\circ$ $L_{GN} = 3.3E-4 \text{ sr}^{-1}$

$$L_{GN}(\theta_0, \theta, \varphi, \sigma^2) = \frac{\rho(\omega)}{4} P(\theta_0, \theta, \varphi, \sigma^2) \frac{(1 + \tan^2 \beta)^2}{\cos \theta}$$

L_{GN} : normalized sunglint reflectance (unit: sr^{-1}), derived from Cox-Munk model.



Sunglint requirement for UV detection

6 Future research plan

- Work on the atmospheric correction of UV band.
- Study the UV reflection characteristics and mechanism of other sea surface targets (e.g., sea ice).



- Detection of oil spills using **ultraviolet remote sensing**
- Detection of oil spills using **Landsat-8 OLI data**

Xiaorun Hong ^{1,†} , Lusheng Chen ^{2,†}, Shaojie Sun ^{2,3,4,5,*} , Zhen Sun ⁶, Ying Chen ², Qiang Mei ⁷
and Zhichao Chen ²

¹ School of Geography and Planning, Sun Yat-sen University, Guangzhou 510006, China

² School of Marine Sciences, Sun Yat-sen University, Zhuhai 519082, China

³ Southern Marine Science and Engineering Guangdong Laboratory (Zhuhai), Zhuhai 519000, China

⁴ Guangdong Provincial Key Laboratory of Marine Resources and Coastal Engineering,
Guangzhou 510275, China

⁵ Pearl River Estuary Marine Ecosystem Research Station, Ministry of Education, Zhuhai 519000, China

⁶ School of Marine Engineering and Technology, Sun Yat-sen University, Zhuhai 519082, China

⁷ Navigation College, Jimei University, Xiamen 361021, China

* Correspondence: sunshj7@mail.sysu.edu.cn; Tel.: +86-186-6697-2696

† These authors contributed equally to this work.

1 Introduction

■ Objectives

- How are the oil spill distributed in the northern South China Sea?
- What are the sources of the discharged oil?

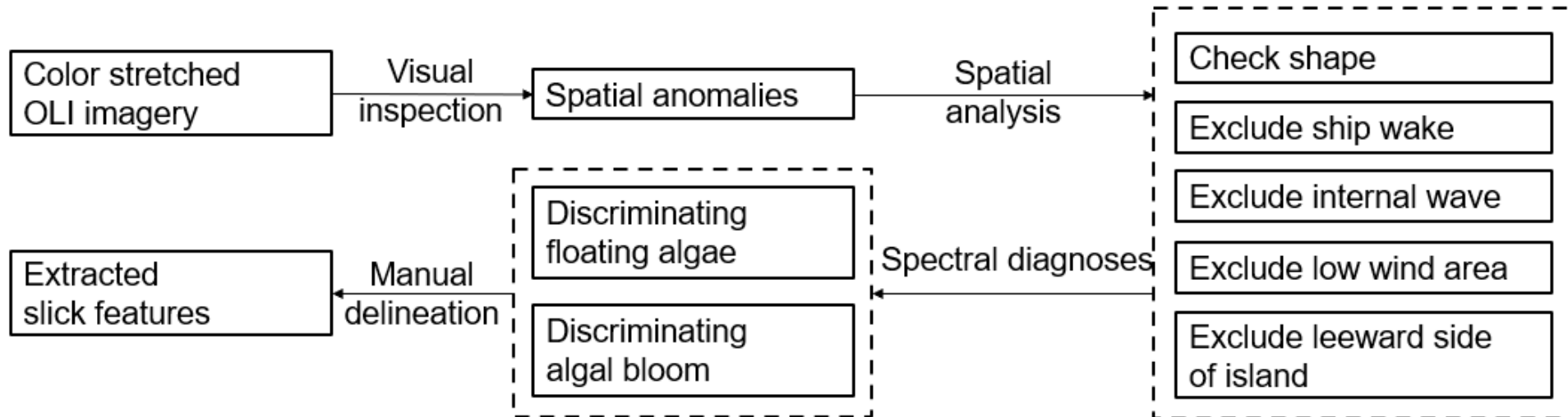
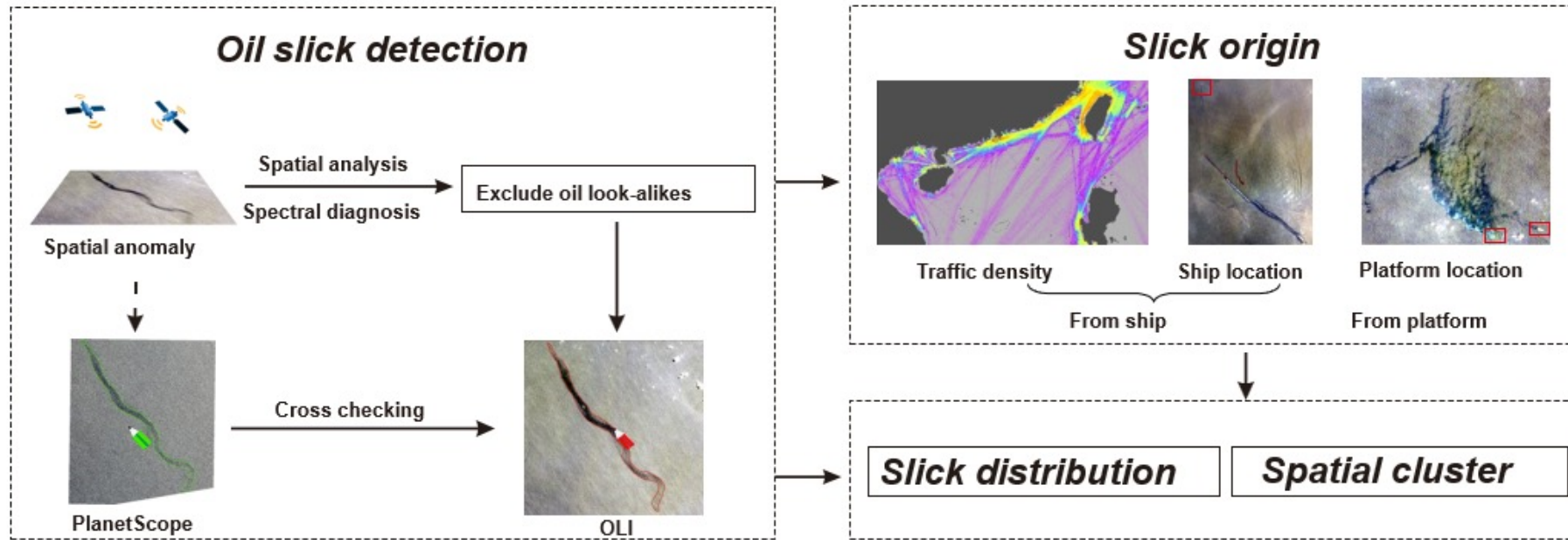
■ Problems

- Small sized oil spills are often overlooked
- According to ITOPF(International Tanker Owners Pollution Federation Limited), >80% of oil spill incidents recorded were small spills (<7 tons) since 1970

■ Solutions

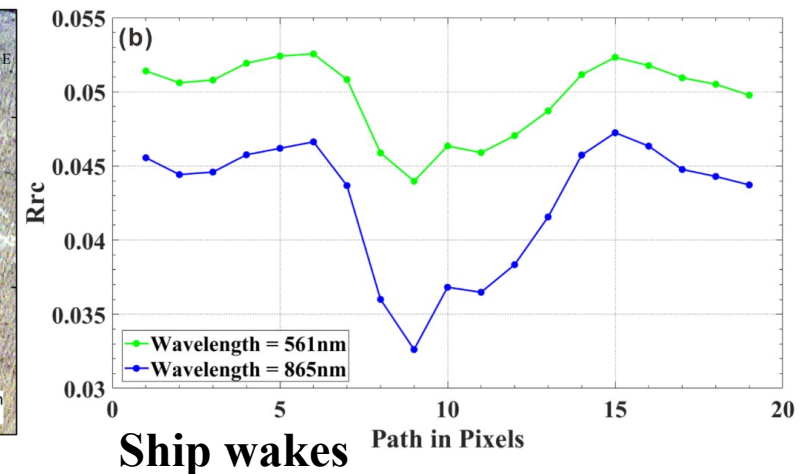
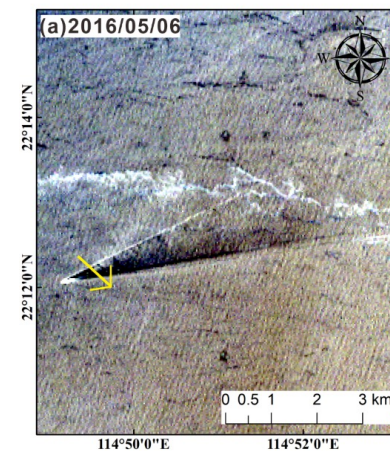
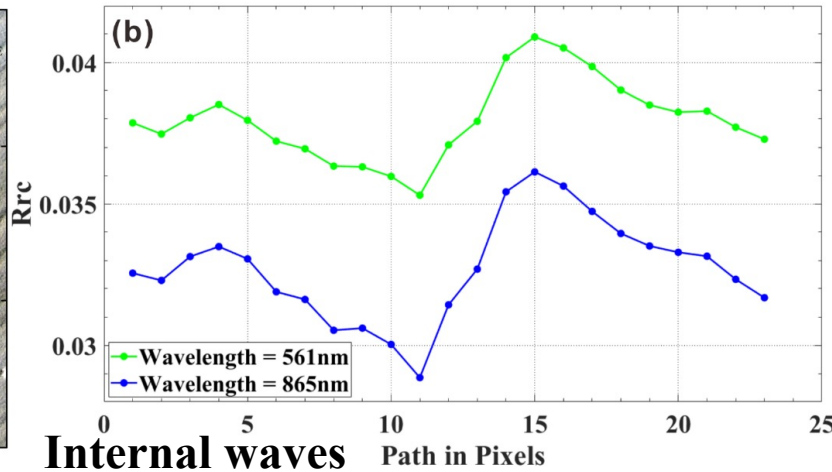
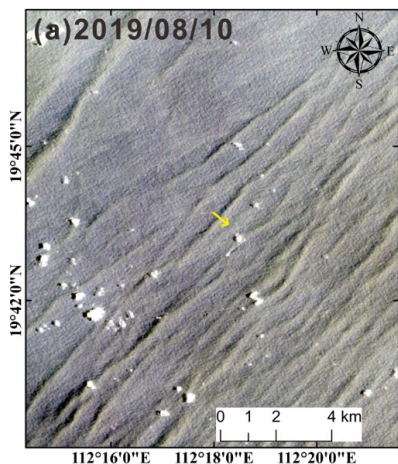
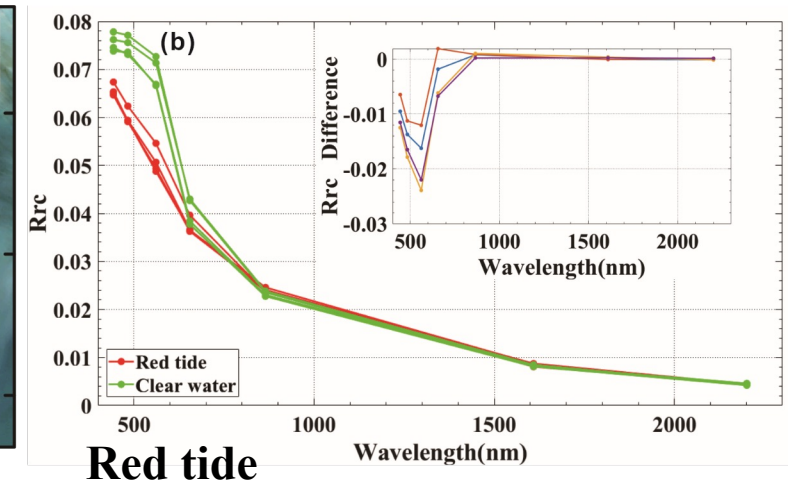
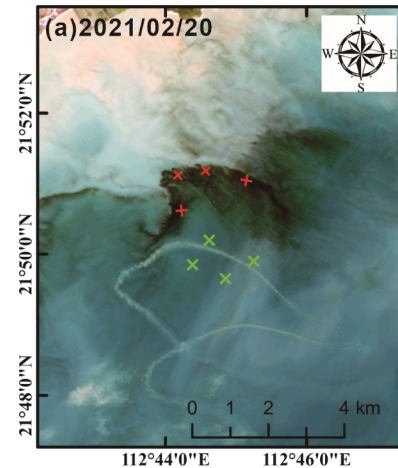
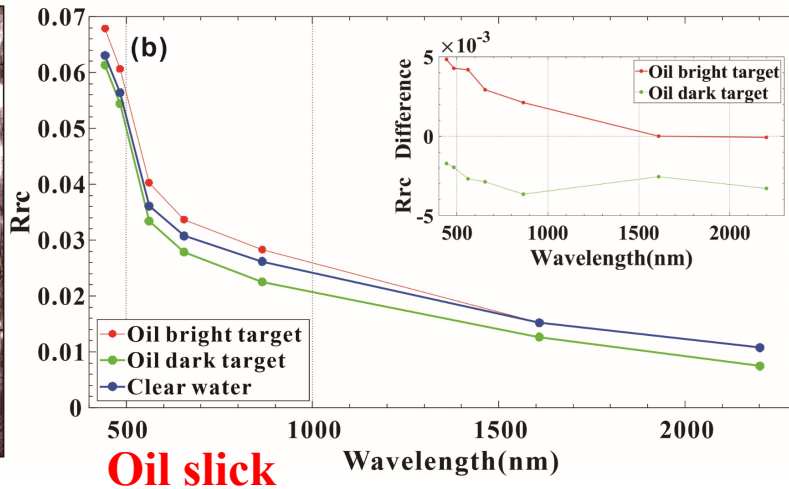
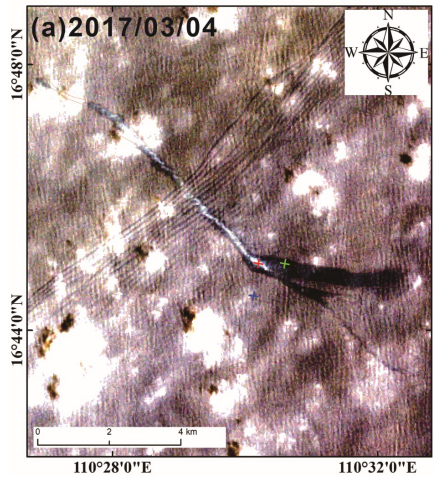
- Detection of oil spills in northern South China Sea using Landsat-8 OLI data

2 Methods



2 Methods

Distinguish between oil slick and oil look-alikes spectrally and spatially



2 Methods

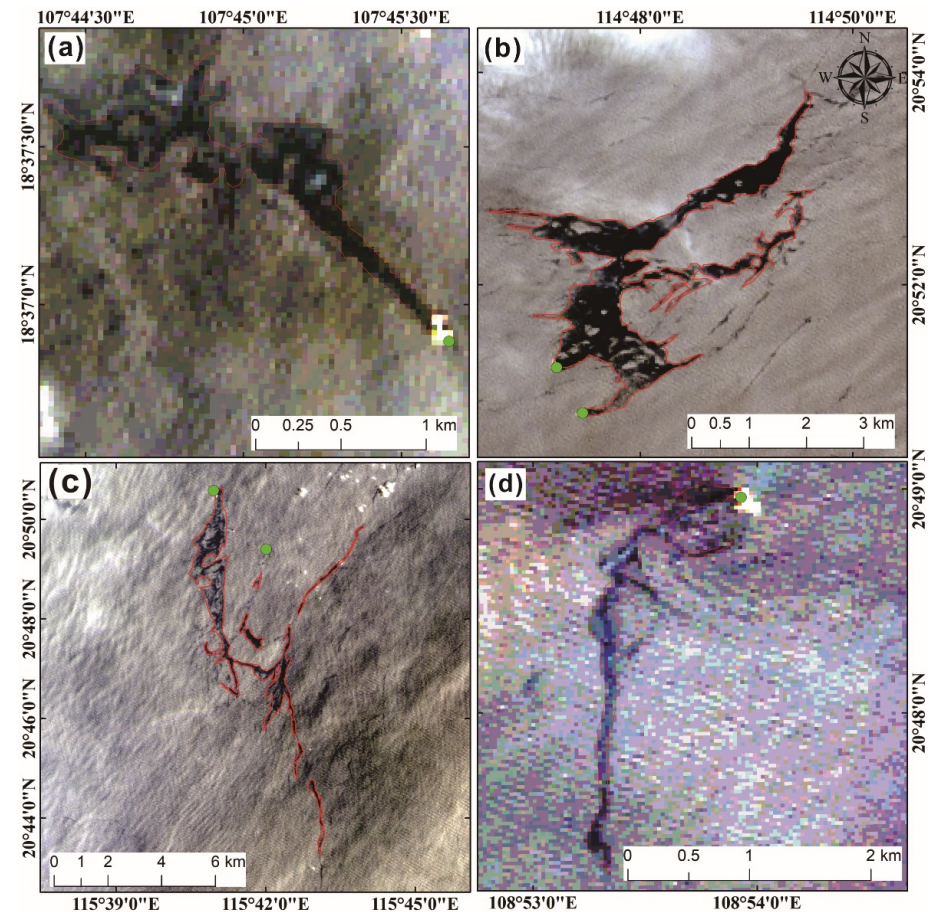
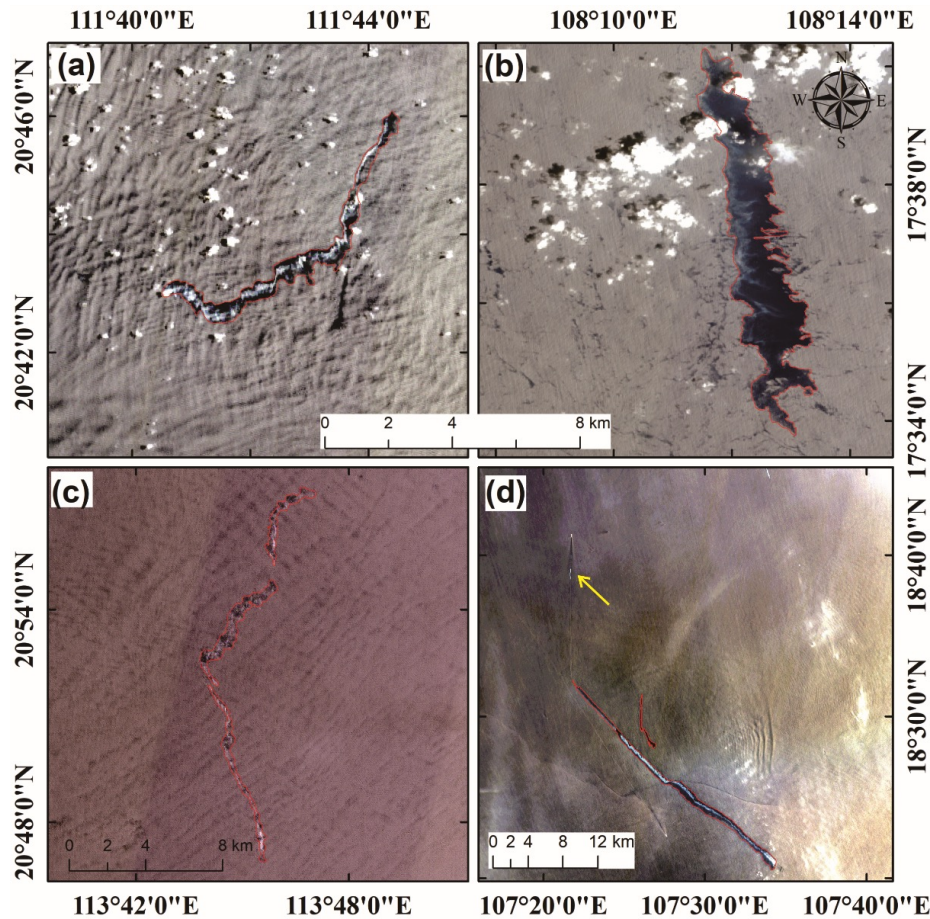
■ Delineated oil slicks

- Ships: traffic density > threshold;
- Platforms: slick attached or nearby;
- Unknowns: others

Sources:

78% from ships

9% from platforms

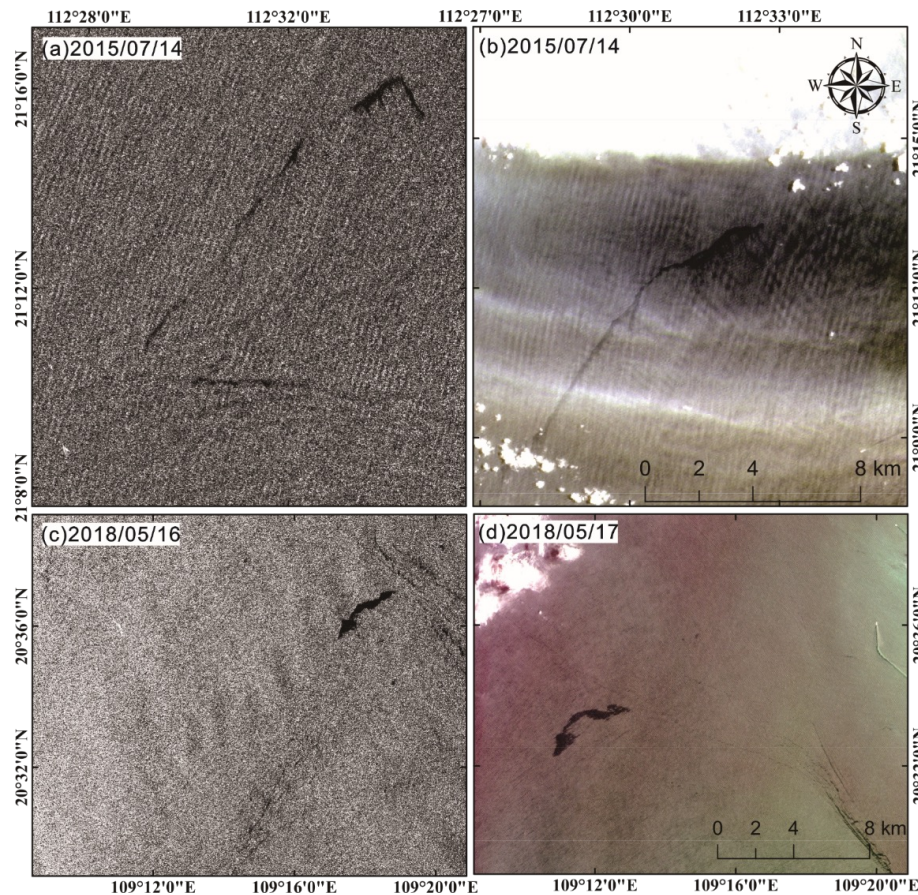


2 Methods

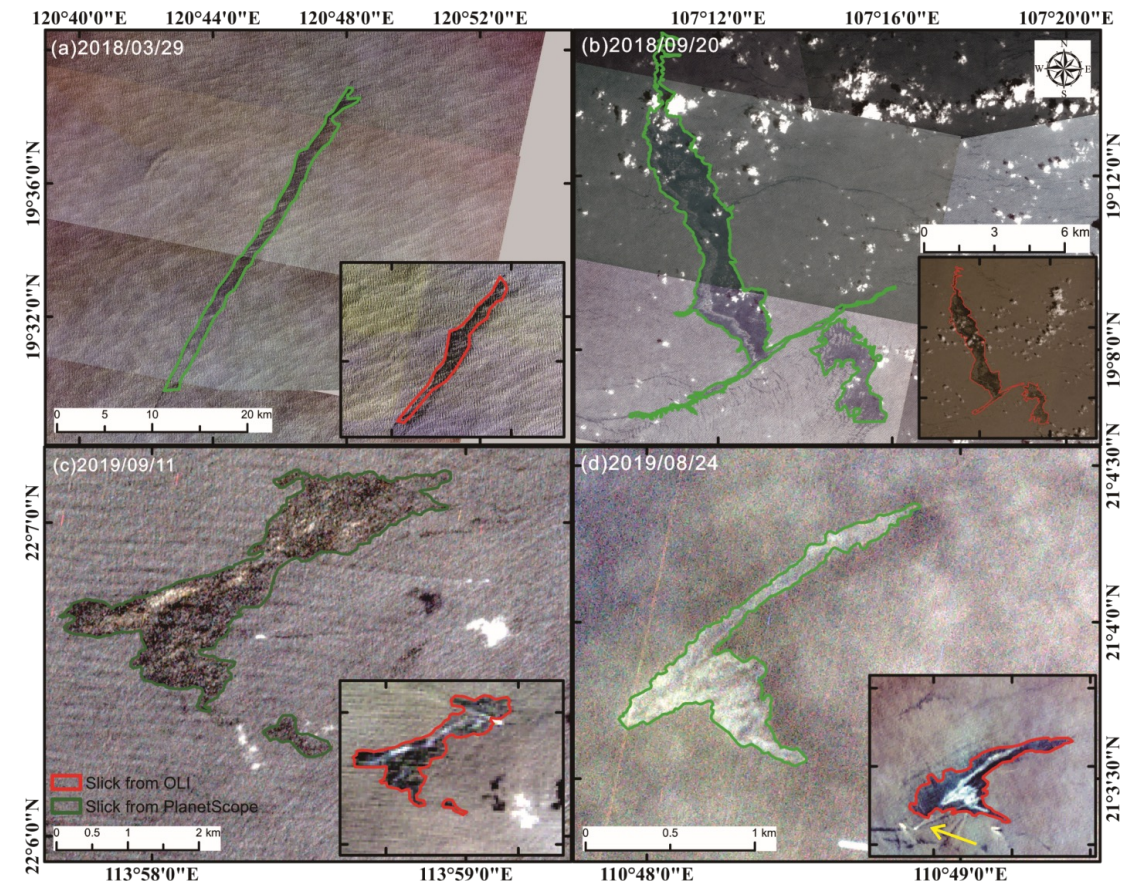
■ Cross-checking

Mean area difference: 17%

OLI vs Sentinel-1 SAR

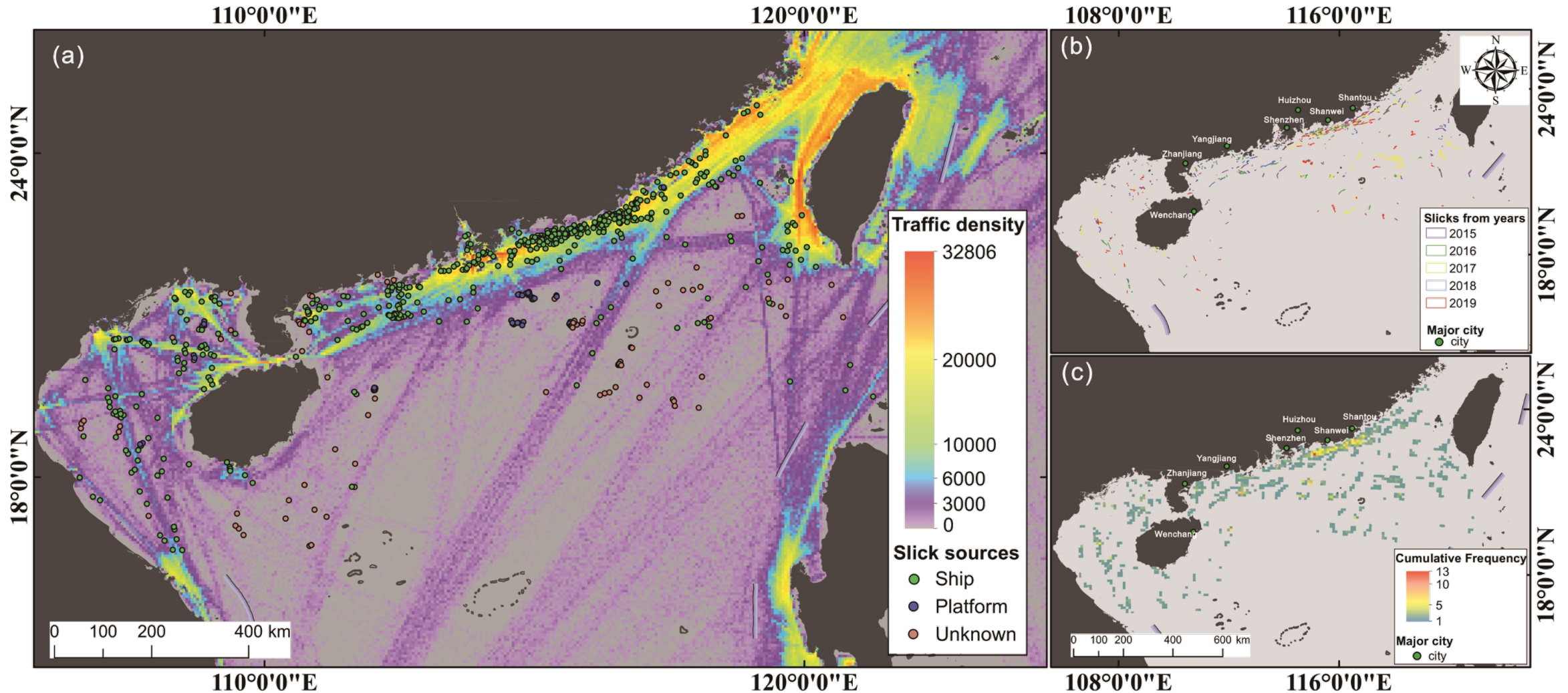


OLI vs PlanetScope



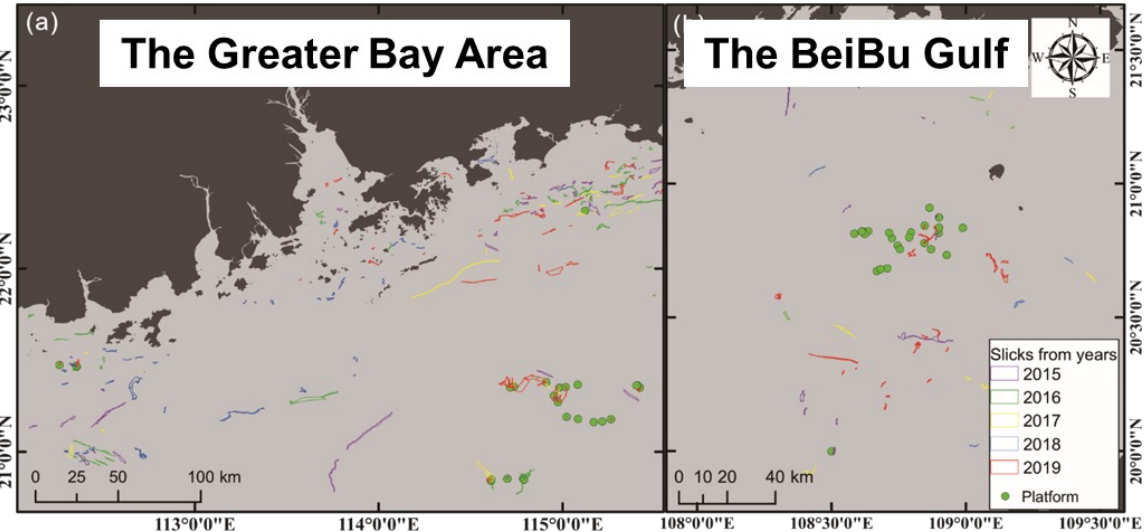
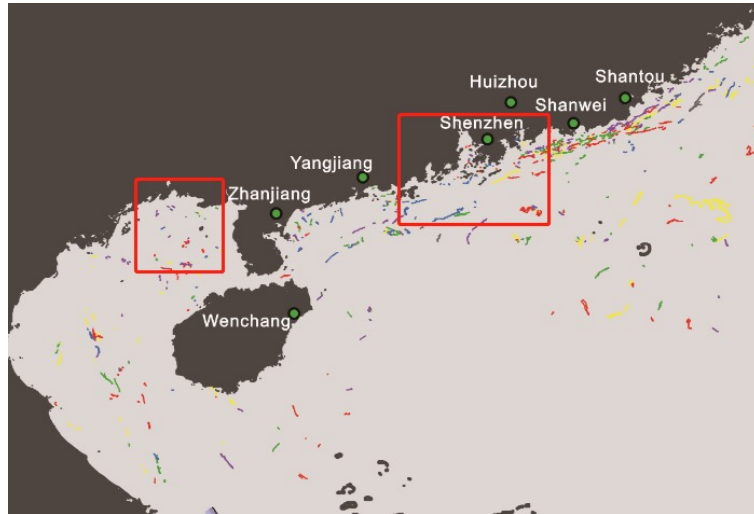
3 Results

■ Distribution of oil slicks in northern South China Sea



3 Results

■ Distribution of oil slicks in northern South China Sea



The Greater Bay Area (GBA)

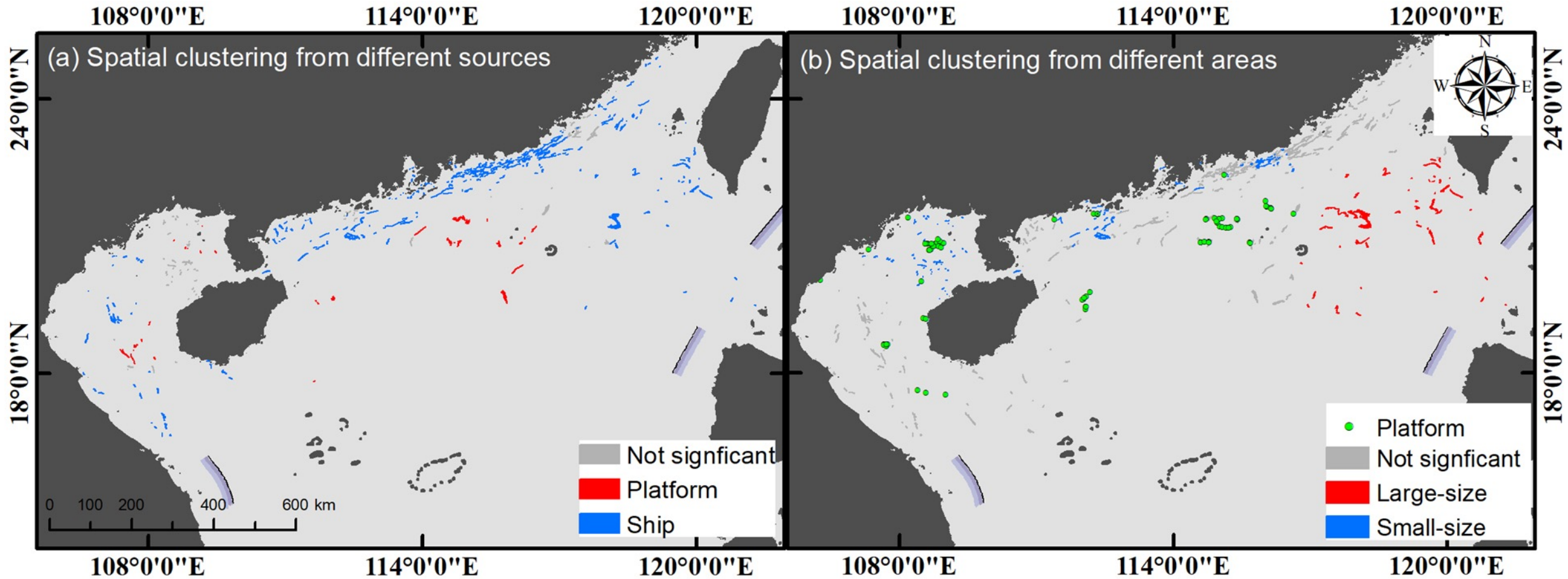
Year	Spring (times)	Summer (times)	Fall (times)	Winter (times)	Total (times)	Maximum area (km ²)	Minimum area (km ²)	Average area (km ²)	Median area (km ²)	Total area (km ²)
2015	27	8	7	0	42	21.1	0.24	3.7	2.0	154.4
2016	17	21	6	0	44	35.5	0.21	3.8	2.0	165.0
2017	3	22	0	2	27	22.7	0.30	3.5	1.1	94.3
2018	25	21	0	0	46	26.9	0.21	2.7	1.0	124.8
2019	22	0	13	4	39	33.8	0.21	4.4	2.1	170.0

The BeiBu Gulf

Year	Spring (times)	Summer (times)	Fall (times)	Winter (times)	Total (times)	Maximum area (km ²)	Minimum area (km ²)	Average area (km ²)	Median area (km ²)	Total area (km ²)
2015	9	0	0	5	14	9.1	0.25	1.6	0.8	23.3
2016	6	0	0	1	7	2.9	0.36	1.1	0.5	7.8
2017	0	3	0	3	6	3.6	0.34	1.5	1.2	9.3
2018	2	4	0	0	6	2.4	0.24	1.0	0.6	6.1
2019	6	1	10	0	17	4.7	0.22	1.4	0.6	24.0

3 Results

Oil spill spatial distribution patterns through spatial cluster analysis





4 Conclusions

- An cumulative oil pollution of 3,242 km² in the NSCS from 2015 to 2019
- Average area of detected slicks was 4.8 km², with half of the slick area <1.7 km²
- 90% of the oil spills were within 112 km of the shoreline, and half of the slicks within 33 km from shorelines
- Slicks from ship or unknown sources tended to have larger areas than slicks from platforms

- Introduction of the project's information
- Recent progress of the project
 1. Optical remote sensing image preprocessing
 2. Oil spills detection
 3. Water quality parameter retrieving

- Spatiotemporal analysis of water clarity in inland waters across Hainan Island
- Spatiotemporal analysis of Chlorophyll-a concentration in Lake Taihu

Ruiting Qiu ^{1,2}, Shenglei Wang ^{2,3,*}, Jiankang Shi ⁴, Wei Shen ¹, Wenzhi Zhang ^{2,3,5}, Fangfang Zhang ^{2,3} 
and Junsheng Li ^{2,3,5} 

¹ School of Earth Science and Resources, China University of Geoscience, Beijing 100083, China

² Key Laboratory of Digital Earth Science, Aerospace Information Research Institute, Chinese Academy of Sciences, Beijing 100094, China

³ International Research Center of Big Data for Sustainable Development Goals, Beijing 100094, China

⁴ Center of Ecology Environment Monitoring of Hainan Province, Haikou 571126, China

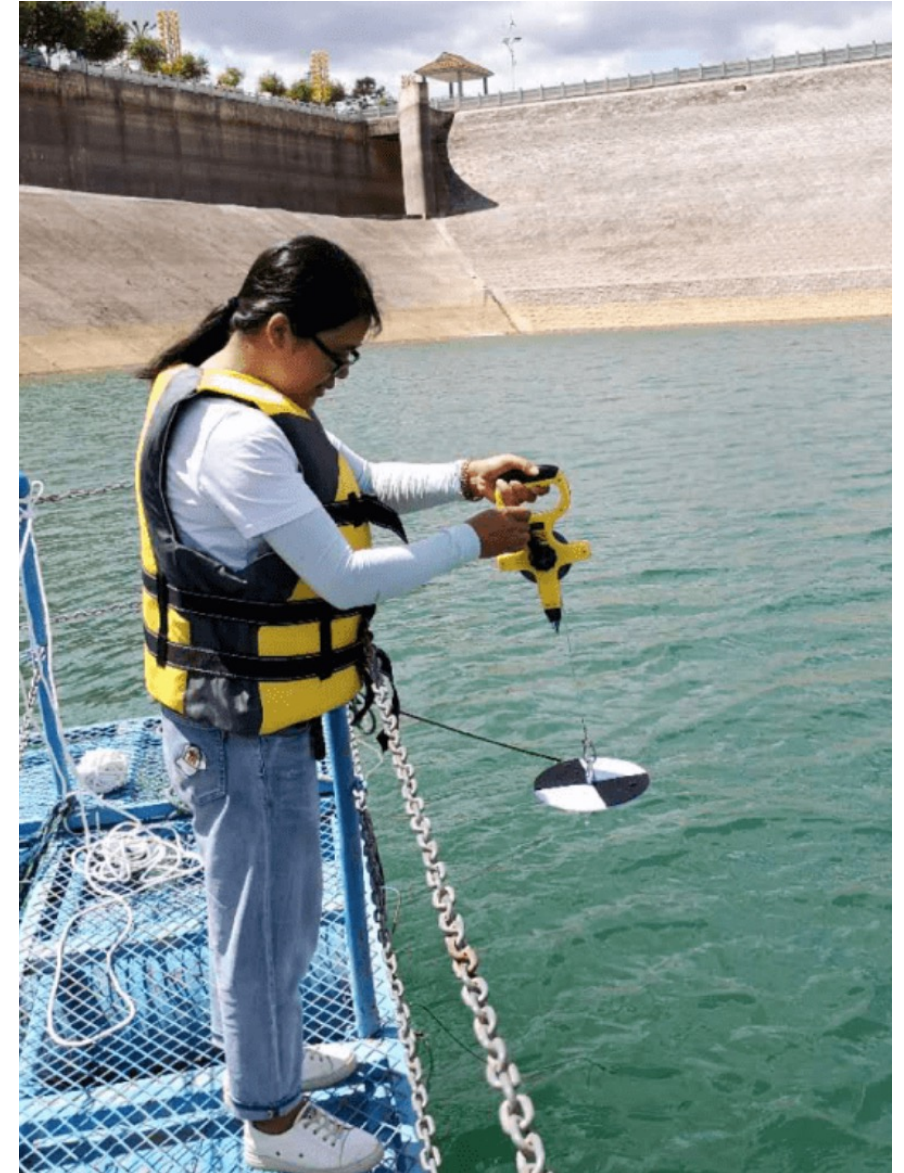
⁵ University of Chinese Academy of Sciences, Beijing 100049, China

* Correspondence: wangsl@radi.ac.cn

1 Introduction

- **Water clarity (Secchi disk depth, Z_{SD})**
 - Simple and cost-effective measurement
 - An important indicator of light propagation in water
 - An important indicator of lake ecosystem

- **Water clarity monitoring for regional small water bodies using high spatial resolution satellite data is important to SDG6 evaluation and understand the status and changes of water bodies.**



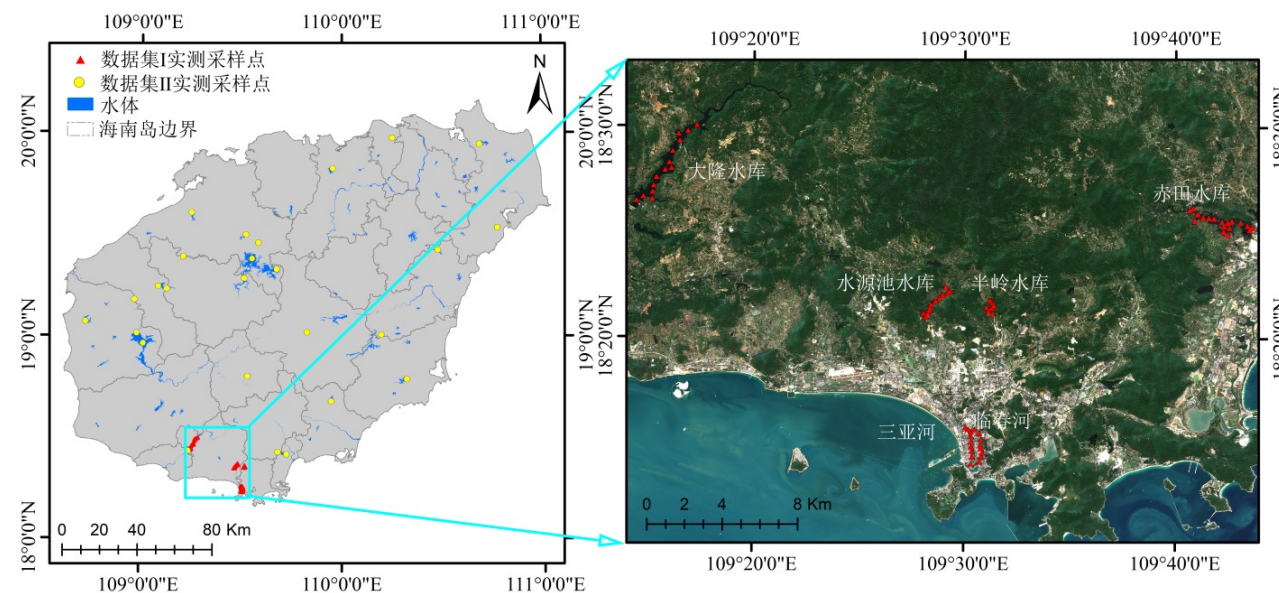
1 Introduction

- Hainan Island has plenty of freshwater resources, but most of the water bodies are small artificial reservoirs that the area is less than 10 km².
- With the acceleration of urbanization, the lakes and reservoirs in the Hainan Island are facing increasingly serious water pollution problems, such as industrial pollution, domestic sewage, and other water pollution.
- On the other hand, the construction of the ‘Hainan Free Trade Port’ proposed in 2018 and as a distinctive provincial demonstration area in China for SDG implementation proposed in 2021, has further promoted protection of the hydro-ecological environment on the Hainan Island.



2 Study area and data description

- ◆ **Study area:** 71 small water bodies across Hainan Island
- ◆ **Time period:** 2017-2021
- ◆ **Satellite data:** Sentinel-2 MSI
- ◆ **In situ data**



Dataset I: The in situ experiment dataset in several water bodies in Sanya City.

Dataset II: The routine water quality monitoring data from Hainan government.

3 Methods

Satellite data preprocessing

- Water boundary identification

Method: NDWI+OTSU

- Remote Sensing Reflectance Correction

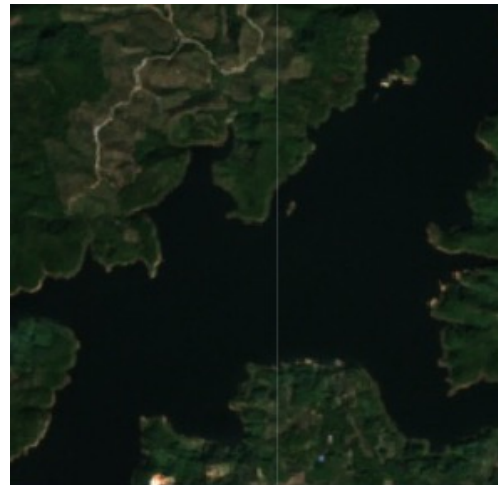
$$R_{rs}(\lambda) = \frac{R(\lambda) - \min(R_{NIR} : R_{SWIR})}{\pi}$$



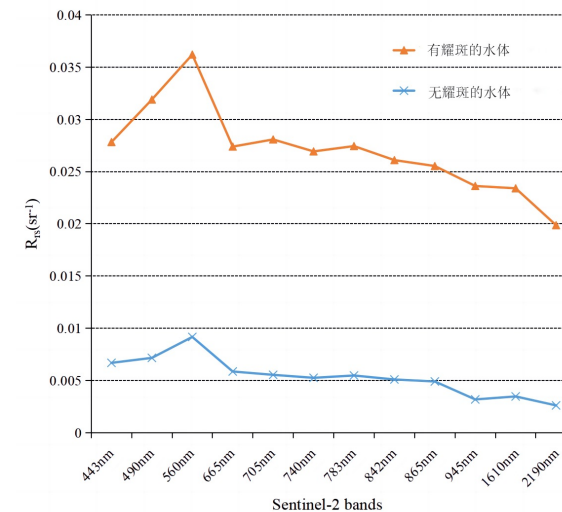
Water boundary identification



Water with sun glint



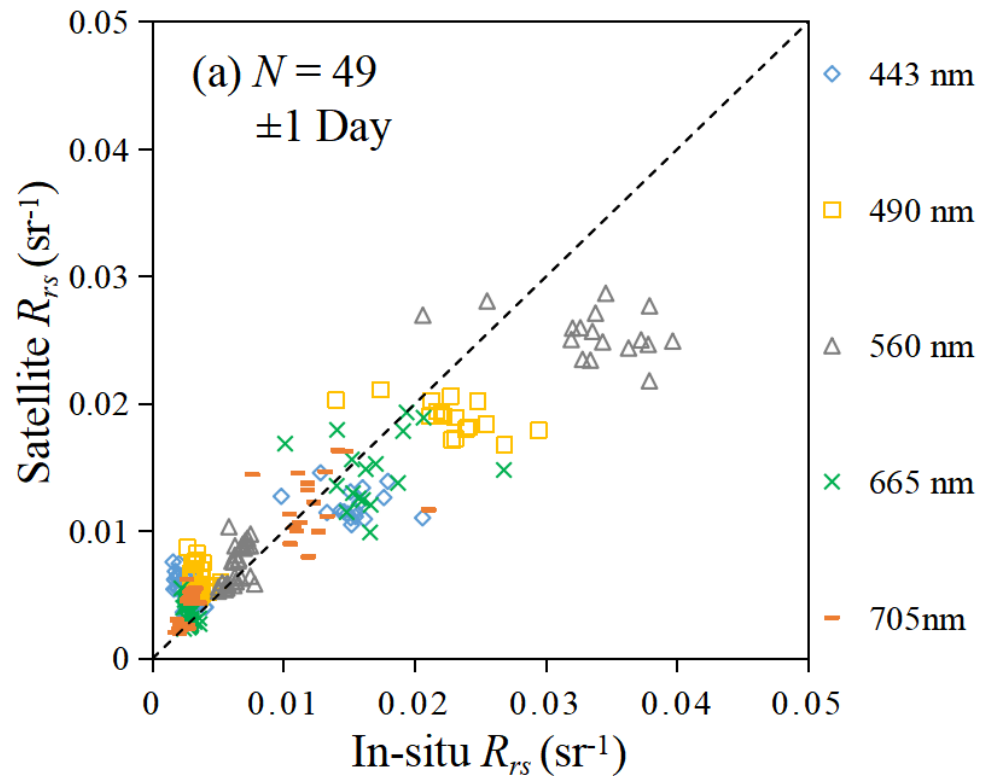
Water without sun glint



3 Methods

Satellite data preprocessing

Comparison between the synchronous in situ measured $R_{rs}(\lambda)$ and Sentinel-2 MSI $R_{rs}(\lambda)$.



Band	R^2	MRE	RMSE
443nm	0.88	29.2%	0.0000099415
490nm	0.88	26.8%	0.0000179022
560nm	0.91	18.9%	0.0000510418
665nm	0.83	16.3%	0.0000107690
705nm	0.80	16.9%	0.0000061268

3 Methods

Water clarity (Z_{SD}) estimation model development

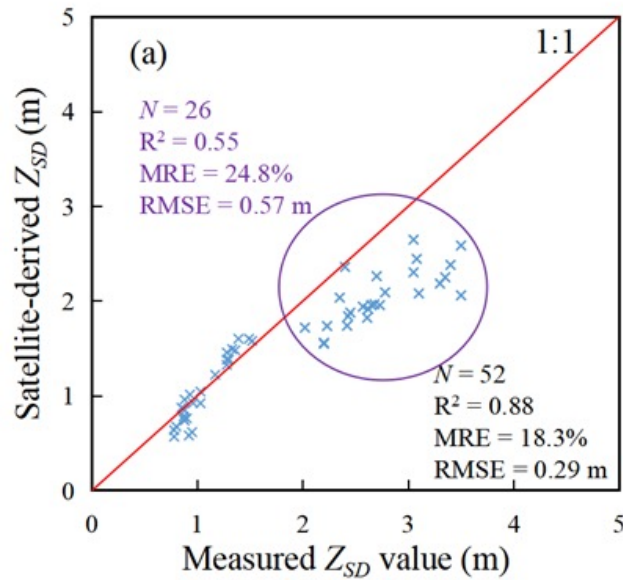
QAA-v6m based semi-analytical model

a new threshold value of $R_{rs}(665)$, i.e. 0.005, was proposed for distinguishing the clear and turbid waters.

Step 1: Classifying water bodies with $R_{rs}(665)$	$r_{rs}(\lambda) = R_{rs}(\lambda)(0.52 + 1.7R_{rs}(\lambda))$	
	A new threshold $u(\lambda) = \frac{-g_0 + \sqrt{(g_0)^2 + 4g_1 * r_{rs}(\lambda)}}{2g_1}$, where $g_0 = 0.089$ and $g_1 = 0.1245$	
	IF $R_{rs}(665) < 0.005 \text{ sr}^{-1}$(QAA_clear)	IF $R_{rs}(665) \geq 0.005 \text{ sr}^{-1}$(QAA_turbid)
	2 $\chi = \log \left(\frac{r_{rs}(443) + r_{rs}(490)}{r_{rs}(560) + 5 \frac{r_{rs}(665)}{r_{rs}(490)} r_{rs}(665)} \right)$ $\alpha(\lambda_0) = \alpha(560) = \alpha_w(\lambda_0) + 10^{h_0 + h_1 \chi + h_2 \chi^2}$	$\alpha(\lambda_0) = \alpha(665) = \alpha_w(665) + 0.39 \left(\frac{R_{rs}(665)}{R_{rs}(443) + R_{rs}(490)} \right)^{1.14}$
	3 $b_{bp}(\lambda_0) = b_{bp}(560) = \frac{u(\lambda_0) \times \alpha(\lambda_0)}{1 - u(\lambda_0)} - b_{bw}(560)$	$b_{bp}(\lambda_0) = b_{bp}(665) = \frac{u(\lambda_0) \times \alpha(\lambda_0)}{1 - u(\lambda_0)} - b_{bw}(665)$
Step 2: Deriving a and b_b with QAA_v6	4 $\eta = 2.0 \left(1 - 1.2 \exp \left(-0.9 \frac{r_{rs}(443)}{r_{rs}(560)} \right) \right)$	
	5 $b_{bp}(\lambda) = b_{bp}(\lambda_0) \left(\frac{\lambda_0}{\lambda} \right)^\eta$	
	6 $\alpha(\lambda) = (1 - u(\lambda))(b_w(\lambda) + b_{bp}(\lambda)) / u(\lambda)$	
Step 3: Derived Z_{SD}	7 $K_d(\lambda) = (1 + m_0 \times \theta_s) \alpha(\lambda) + \left(1 - \gamma \frac{b_{bw}(\lambda)}{b_b(\lambda)} \right) \times m_1 \times (1 - m_2 \times e^{-m_3 \times \alpha(\lambda)}) b_b(\lambda)$	
	8 $Z_{SD} = \frac{1}{2.5 \text{Min}(K_d(443, 490, 560, 665))} \ln \left(\frac{0.14 - R_{rs}^v}{0.013} \right)$	

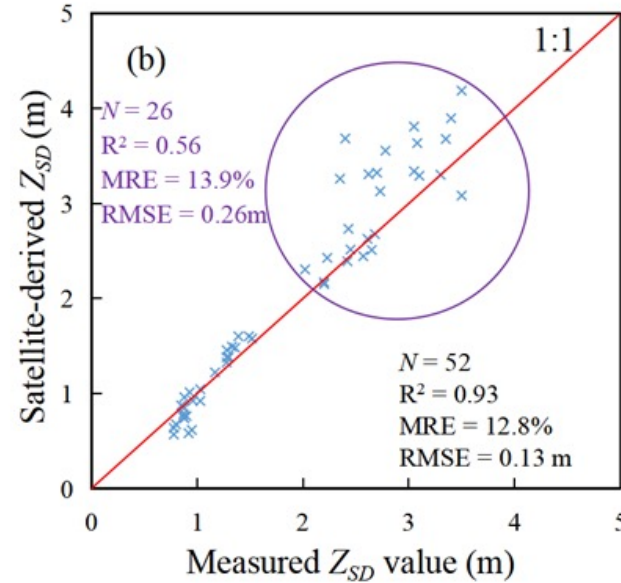
3 Methods

Water clarity (Z_{SD}) estimation model evaluation

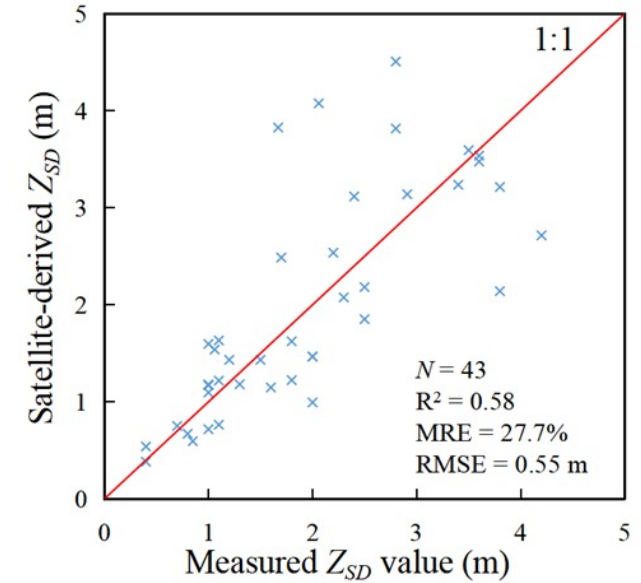


(a) The Z_{SD} -QAAv6 model

Validation of the model using Dataset I



(b) The Z_{SD} -QAAv6m model.



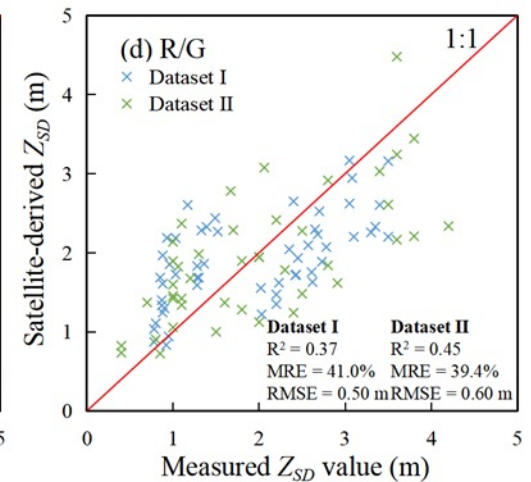
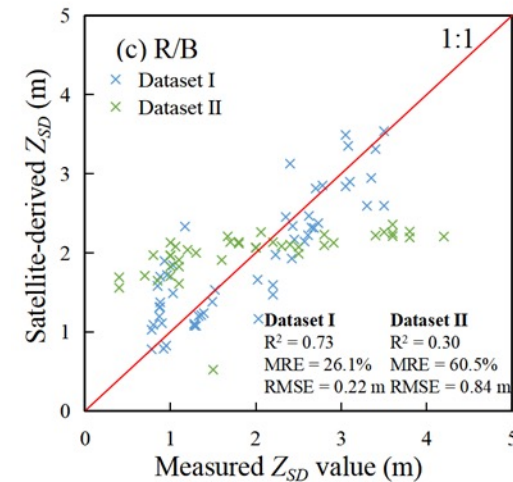
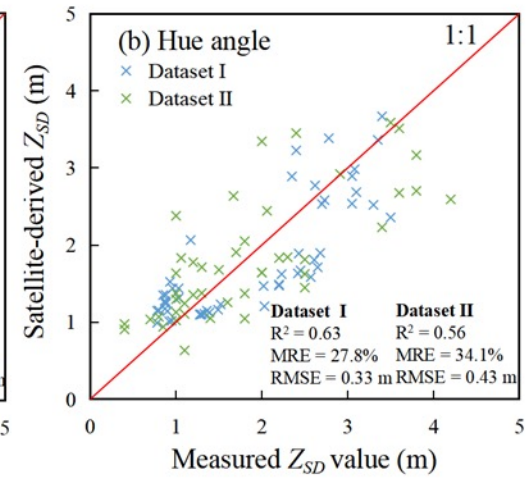
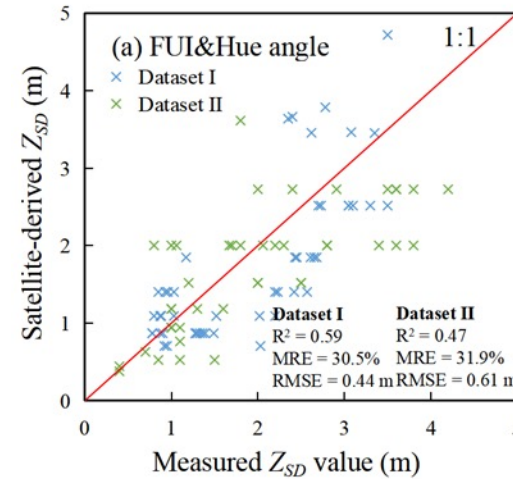
Validation of the model using Dataset II

QAA-v6m based model performed better ($R^2 = 0.93$, $MRE = 12.8\%$, $RMSE = 0.13$ m), which can solve the underestimation in Z_{SD} -QAAv6 model when Z_{SD} is above 2 m.

3 Methods

Water clarity (Z_{SD}) estimation model comparison

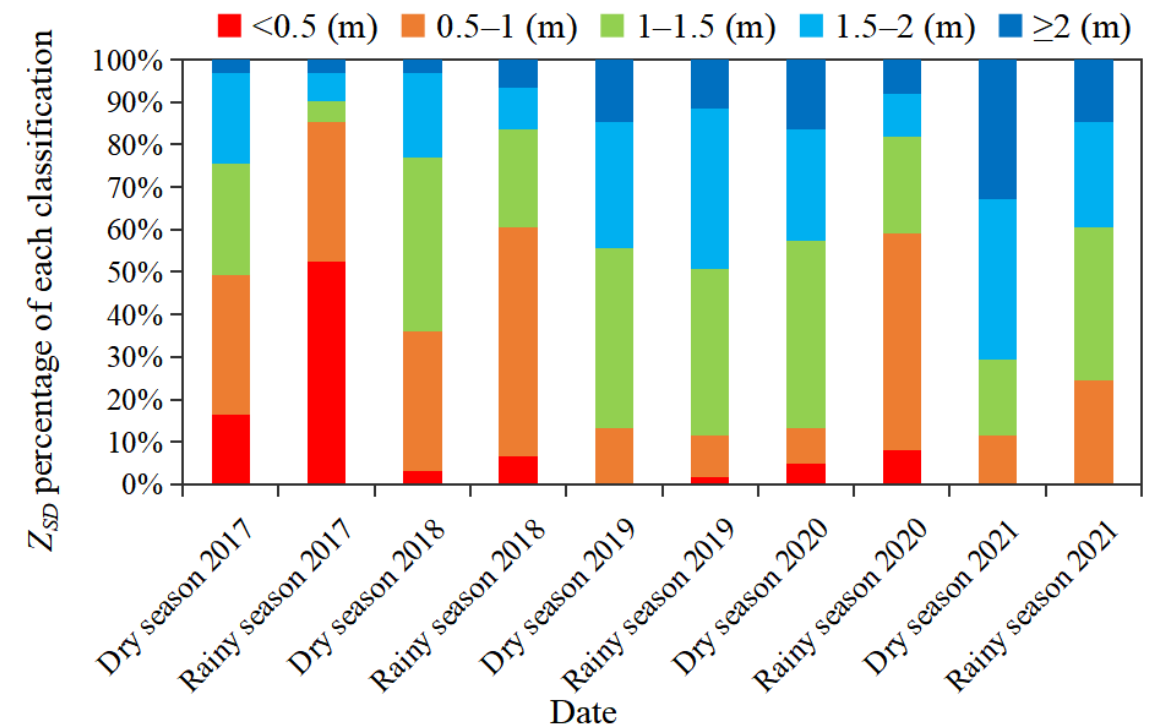
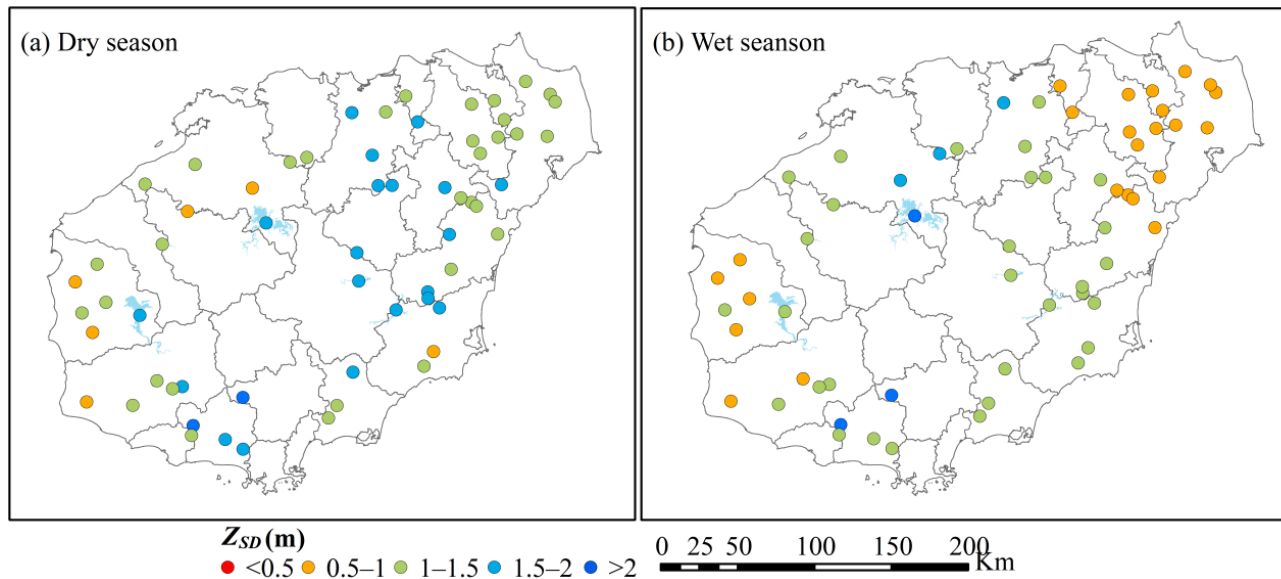
The modified QAA-v6m based semi-analytical model outperformed the empirical models in the Z_{SD} retrieval for inland waters in the Hainan Island using Sentinel-2 data.



4 Results

■ Spatial-temporal changes of water clarity in inland waters across Hainan Island

- **Water clarity is higher in dry season and lower in wet season.**
- **Water clarity is increasing across Hainan Island.** From 2017–2021, the proportion of water bodies with higher Z_{SD} values (≥ 1.5 m) had a significant increase, and the proportion of water bodies with lower Z_{SD} values (< 0.5 m) had a significant increase

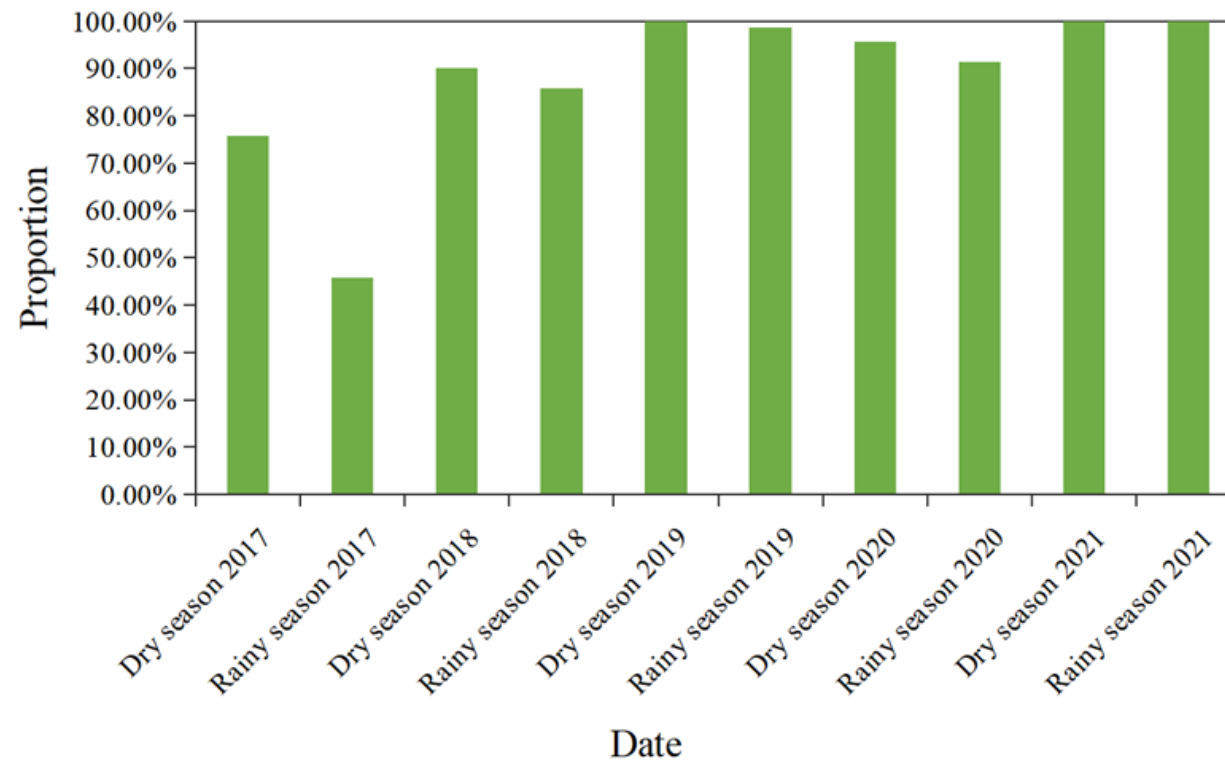


4 Results

■ SDG6.3.2 evaluation based on water clarity

From 2017 to 2021, the proportion of waterbodies with water clarity > 0.5 m increased from 60% to 100%.

There was a significant increase in the proportion of water bodies with good water quality.



proportion of water bodies with water clarity > 0.5 m

5 Conclusions

- **The modified QAA-v6m based semi-analytical model outperformed the empirical models in retrieval of water clarity in inland waters across Hainan Island.**
- **The water clarity in inland waters across Hainan Island generally improved from 2017–2021.**

- Spatiotemporal analysis of water clarity in inland waters across Hainan Island
- Spatiotemporal analysis of Chlorophyll-a concentration in Lake Taihu



ELSEVIER

Contents lists available at [ScienceDirect](https://www.sciencedirect.com)

Science of the Total Environment

journal homepage: www.elsevier.com/locate/scitotenv

Increase in chlorophyll-a concentration in Lake Taihu from 1984 to 2021 based on Landsat observations

Ziyao Yin ^{a,b}, Junsheng Li ^{a,c,d,*}, Bing Zhang ^{a,b}, Yao Liu ^e, Kai Yan ^{a,b}, Min Gao ^{a,f}, Ya Xie ^{a,f}, Fangfang Zhang ^{a,c}, Shenglei Wang ^{a,c}

^a Key Laboratory of Digital Earth Science, Aerospace Information Research Institute, Chinese Academy of Sciences, Beijing 100094, China

^b College of Resources and Environment, University of Chinese Academy of Sciences, Beijing 100049, China

^c International Research Center of Big Data for Sustainable Development Goals, Beijing 100094, China

^d School of Electronic, Electrical and Communication Engineering, University of Chinese Academy of Sciences, Beijing 100049, China

^e Land Satellite Remote Sensing Application Center, Ministry of Natural Resources of China, Beijing 100048, China

^f School of Earth Science and Resources, China University of Geosciences (Beijing), Beijing 100083, China

1 Introduction

■ Challenges

- SPM signals are strong in turbid waters and can interfere with Chla signals;
- The wide bandwidth of Landsat can not clearly reflect the spectral characteristics of Chla.

■ Solutions

- Constructing spectral index for water optical classification, excluding highly turbid waters dominated by SPM;
- Chla models were calibrated and validated only in waters with low SPM.

2 Methods

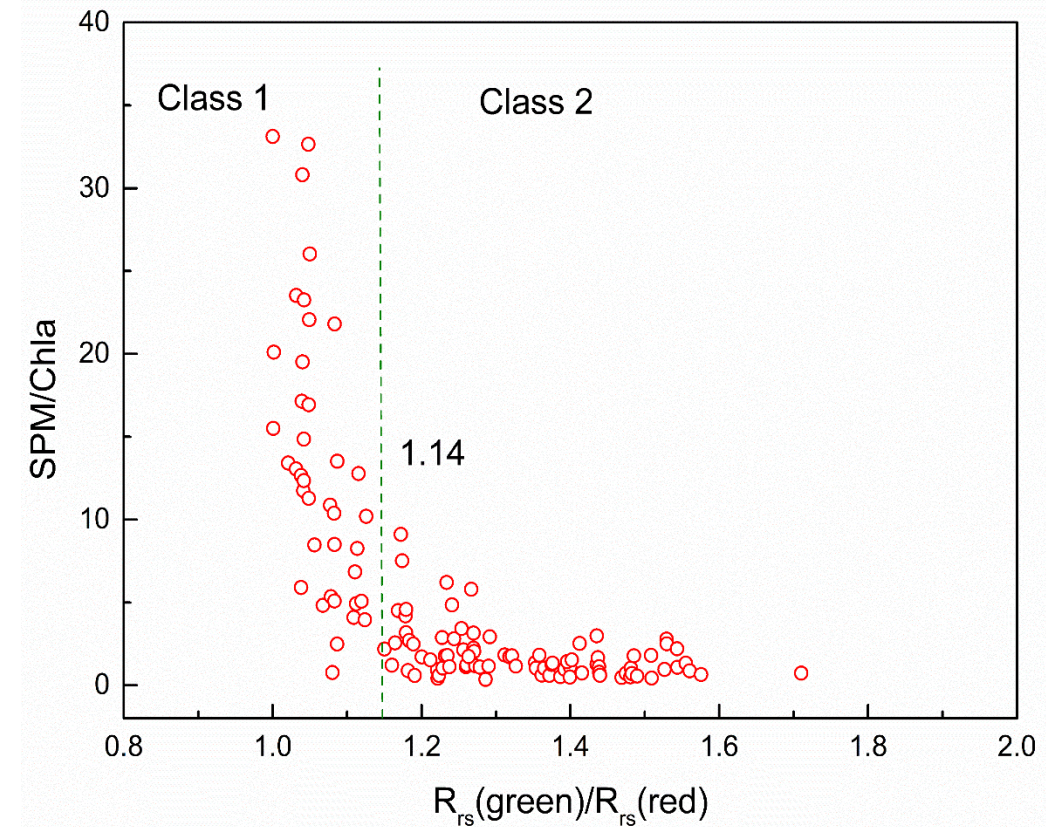
■ Strategy for modeling Chla

➤ Class 1, $R_{rs}(\text{Green})/R_{rs}(\text{Red}) < 1.14$

The SPM/Chla values were high in this class. The optical properties of this type of water were primarily determined by high SPM concentration. Therefore, we considered masking this class and not retrieving Chla.

➤ Class 2, $R_{rs}(\text{Green})/R_{rs}(\text{Red}) \geq 1.14$

The SPM/Chla values were relatively low in this class. This class of water was characterized by a high Chla. Therefore, we considered retaining this class and retrieving Chla.



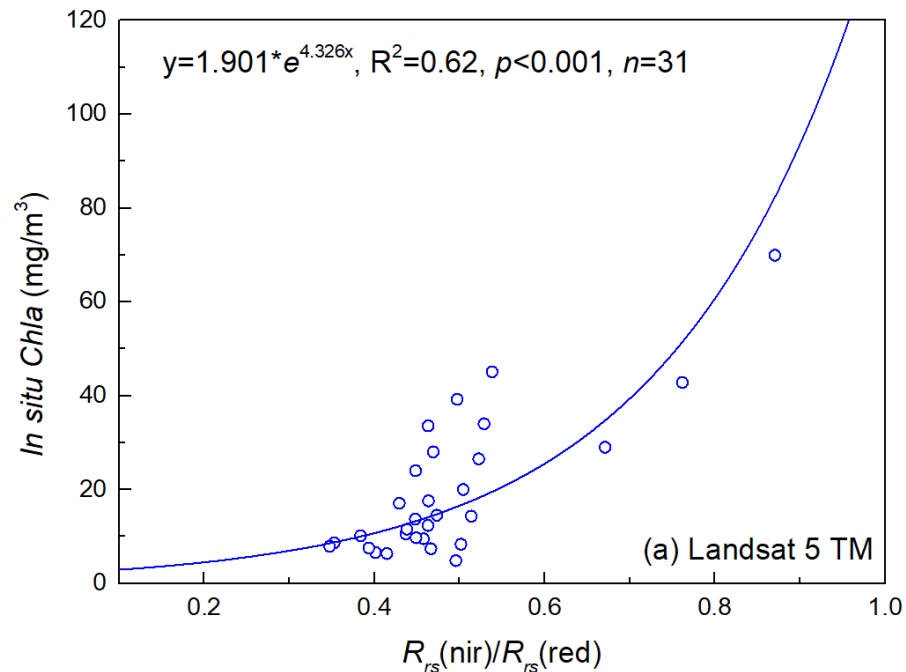
2 Methods

■ Calibration of the Chla model

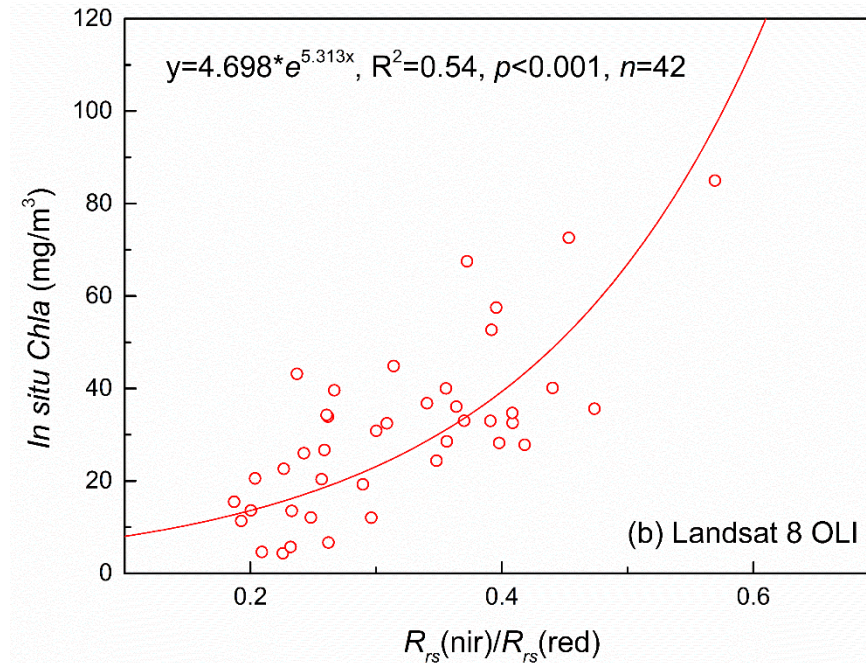
The red edge effect of Chla → high $R_{rs}(nir)$
 High absorption of Chla → low $R_{rs}(red)$



$$R_{rs}(nir)/R_{rs}(red) \propto Chla$$



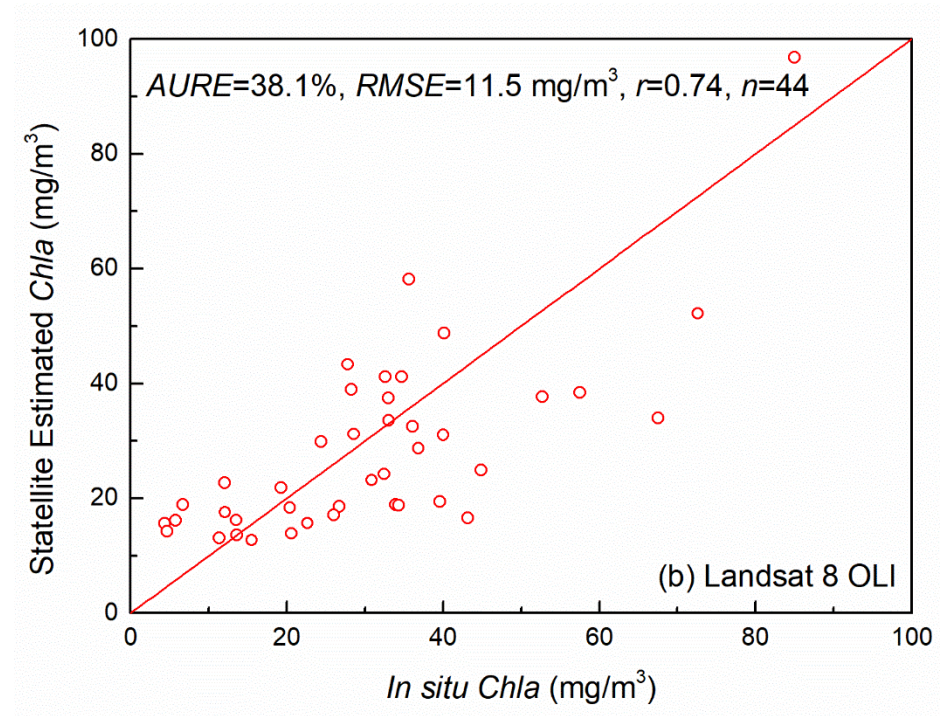
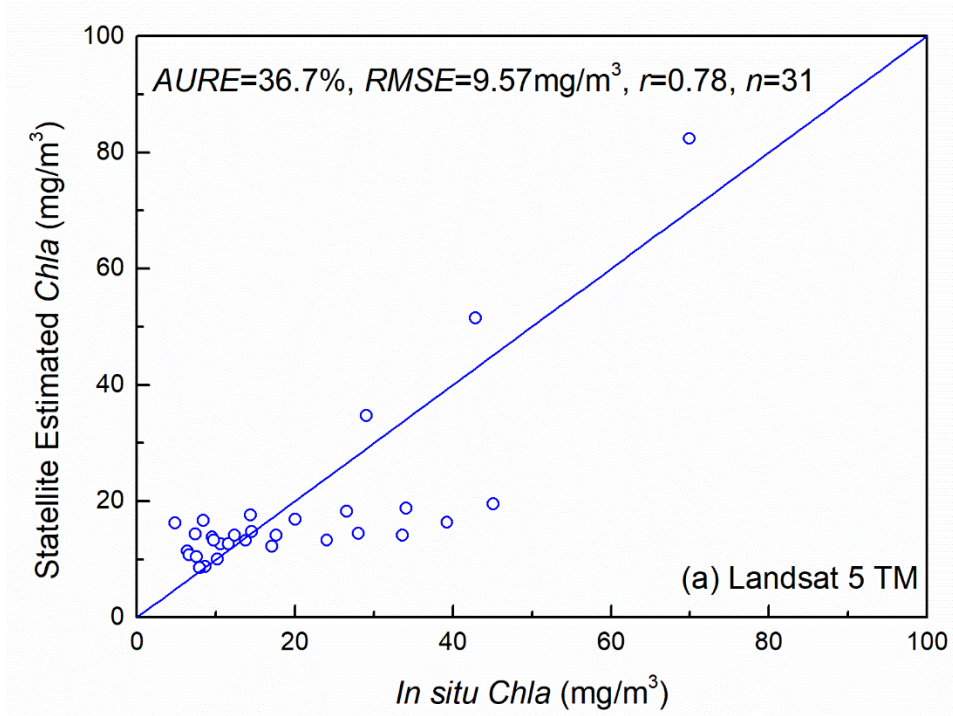
$$Chla_{TM} = 1.901 \times e^{4.326 \times \frac{R_{rs}(nir)}{R_{rs}(red)}}$$



$$Chla_{OLI} = 4.698 \times e^{5.313 \times \frac{R_{rs}(nir)}{R_{rs}(red)}}$$

2 Methods

Validation of the Chla model



Sensor	Average unbiased relative error	root mean square error	correlation coefficient
Landsat TM	36.7%	9.57	0.78
Landsat OLI	38.1%	11.5	0.74

2 Methods

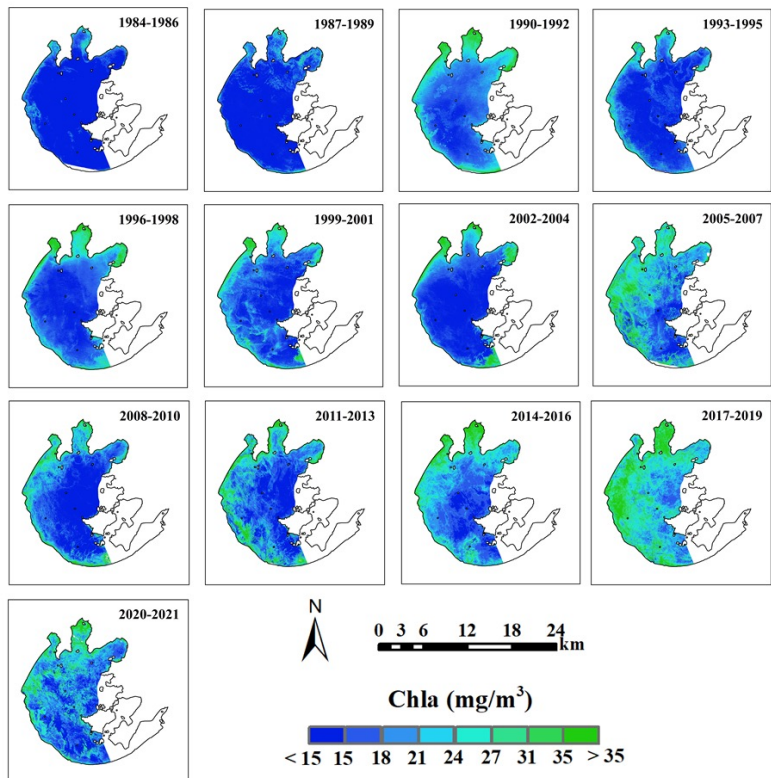
■ Calibration and validation of various Chla models

Reference	Band or spectral index	Calibration		Validation		
		Model	R^2	AURE	r	
Gitelson et al.(1993)	$X=R_{rs}(\text{red})/ R_{rs}(\text{green})$	➤ TM	$\text{Chla}=-49.97*X+59.94$	0.03	62.5%	-0.23
		➤ OLI	$\text{Chla}=30.775*X+7.98$	0.01	111.2%	0.27
Ogashawara et al. (2016)	$X=R_{rs}(\text{red})- R_{rs}(\text{nir})$	➤ TM	$\text{Chla}=57.845*e^{84.91*X}$	0.47	45.1%	0.59
		➤ OLI	$\text{Chla}=87.389*e^{87.64*X}$	0.26	51.2%	0.46
Xing et al. (2016)	$X=R_{rs}(\text{green})+(R_{rs}(\text{green})- R_{rs}(\text{red}))*(\lambda_{\text{nir}}-\lambda_{\text{green}})/(2\lambda_{\text{nir}}-\lambda_{\text{red}}-\lambda_{\text{green}})$	➤ TM	$\text{Chla}=2206.2*X+59.91$	0.34	51.1%	0.46
		➤ OLI	$\text{Chla}=2791.7*X+78.52$	0.29	43.5%	0.45
Schalles et al. (1998)	$X=R_{rs}(\text{red})- R_{rs}(\text{green})-((R_{rs}(\text{nir})- R_{rs}(\text{green})) * (\lambda_{\text{red}} - \lambda_{\text{green}})/(\lambda_{\text{nir}} - \lambda_{\text{green}}))$	➤ TM	$\text{Chla}=1876.7*X-187665$	0.01	62.3%	-0.19
		➤ OLI	$\text{Chla}=1909.4*X+190987$	0.06	49.2%	0.09
Koponen et al. (2007)	$X= R_{rs}(\text{nir})/(R_{rs}(\text{green}) + R_{rs}(\text{red}))$	➤ TM	$\text{Chla}=266.89*X - 37.961$	0.58	42.4%	0.52
		➤ OLI	$\text{Chla}=368.64*X - 18.358$	0.58	40.2%	0.75
Hu et al. (2004)	$X= R_{rs}(\text{blue})/R_{rs}(\text{green})$	➤ TM	$\text{Chla}=48.984*X-18.191$	0.02	63.8%	-0.16
		➤ OLI	$\text{Chla}=-65.776*X+76.659$	0.03	47.4%	-0.10
This study	$X= R_{rs}(\text{nir})/R_{rs}(\text{red})$	➤ TM	$\text{Chla}=1.901*e^{4.326*X}$	0.62	36.7%	0.78
		➤ OLI	$\text{Chla}=4.698*e^{5.313*X}$	0.54	38.1%	0.74

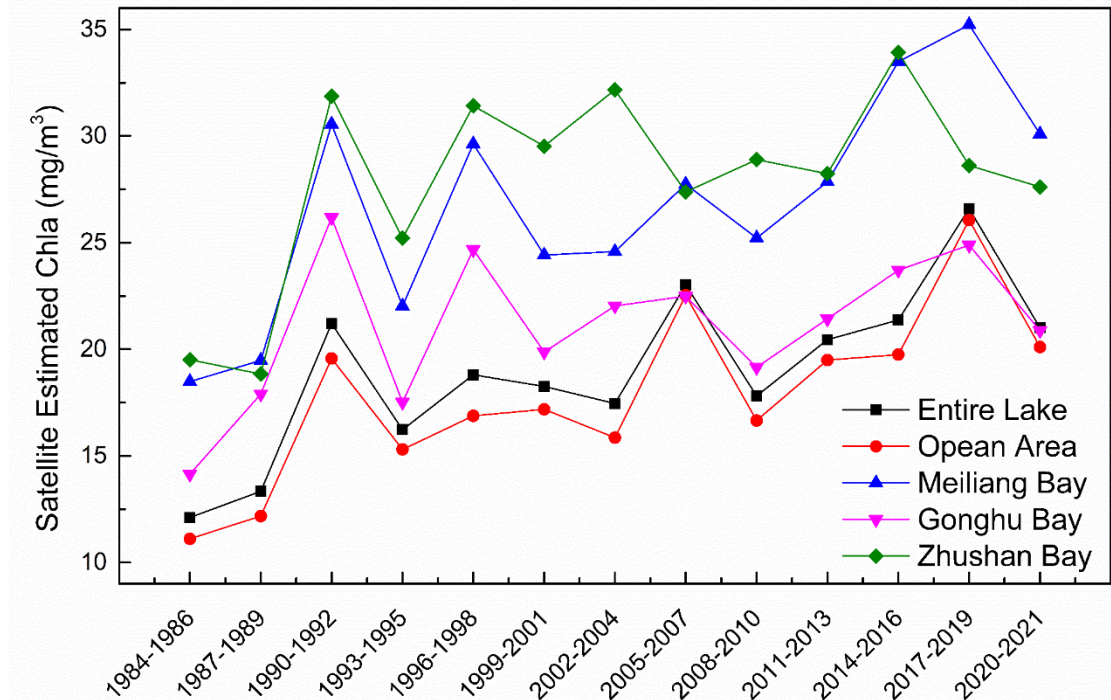
3 Results

■ Spatiotemporal variation of Chla concentrations

- Spatially, Chla were highest in the western and northern regions and lower in the central region of the lake.
- Temporally, an overall significant upward trend of Chla in Lake Taihu was observed from 1984 to 2021.



Spatial distribution of Chla



Temporal distribution of Chla

4 Conclusions

- **A new method was developed for estimating Chla concentrations in Lake Taihu in China, which is primarily characterized by turbidity and eutrophication.**
- **Spatially, Chla concentrations were highest in the western and northern regions and lower in the central region of the lake, which may be attributed to the distribution of rivers flowing into the lake.**
- **Temporally, an overall significant upward trend of Chla in Lake Taihu was observed from 1984 to 2021, which may be primarily caused by an increase in air temperature, decrease in wind speed, and increase in the nutrient content entering the lake.**

- Introduction of the project's information
- Recent progress of the project
 1. Key issues in ocean colour remote sensing
 2. Oil spills detection
 3. Water quality parameter retrieving
- **Summary and outlook**

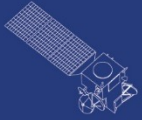
Recent publications

1. Ziyao Yin, Junsheng Li, et al. Increase in chlorophyll-a concentration in Lake Taihu from 1984 to 2021 based on Landsat observations. *Science of the Total Environment*, 2023, 873: 162168.
2. Ruiting Qiu, Shenglei Wang, et al. Sentinel-2 MSI Observations of Water Clarity in Inland Waters across Hainan Island and Implications for SDG 6.3.2 Evaluation. *Remote Sensing*, 2023, 15, 1600.
3. Xiaorun Hong, Lusheng Chen, et al. Detection of Oil Spills in the Northern South China Sea Using Landsat-8 OLI. *Remote Sensing*, 2022, 14, 3966.
4. Ziyi Suo, Ling Li, Yingcheng Lu, et al. Sunlint reflection facilitates performance of spaceborne UV sensor in oil spill detection. *Optics Express*, 2023, 9 (24): 14651.
5. Shaojie Sun, Ying Chen, et al. Optical discrimination of emulsified oil in optically complex estuarine waters. *Marine Pollution Bulletin*, 2022, 184: 114214.
6. Xi Chen, Shaojie Sun. Spectral Discrimination of Pumice Rafts in OpticalMSI Imagery. *Remote Sensing*, 2022, 14, 5854.

Outlook of the 4th year

More work on product scientific and practical value demonstration

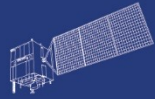
More communications and exchange visits between the Chinese and European partners.



HY



HJ-1AB



CBERS



Gaofen



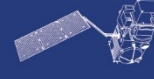
Beijing-2



Sentinel-1



Sentinel-2



Sentinel-3



Sentinel-5p



Aeolus

Thank you

